AGU PUBLICATIONS

Global Biogeochemical Cycles

RESEARCH ARTICLE
10.1002/2015GB005334

**Key Points:**
- Phytoplankton in low-nutrient low-chlorophyll waters near Barbados are phosphate limited
- Atmospheric deposition with high nitrogen and iron relative to phosphorus drives this phosphate limitation
- Prochlorococcus thrives in this environment due to its low phosphorus requirements

**Supporting Information:**
- Supporting Information S1
- Table S2

**Correspondence to:**
A. Paytan,
apaytan@ucsc.edu

**Citation:**
Chien, C.-T., K. R. M. Mackey, S. Dutkiewicz, N. M. Mahowald, J. M. Prospero, and A. Paytan (2016), Effects of African dust deposition on phytoplankton in the western tropical Atlantic Ocean off Barbados, *Global Biogeochem. Cycles*, *30*, 716–734, doi:10.1002/2015GB005334.

Received 15 NOV 2015
Accepted 28 APR 2016
Accepted article online 29 APR 2016
Published online 21 MAY 2016



# Effects of African dust deposition on phytoplankton in the western tropical Atlantic Ocean off Barbados

**Chia-Te Chien[1], Katherine R. M. Mackey[2], Stephanie Dutkiewicz[3], Natalie M. Mahowald[4], Joseph M. Prospero[5], and Adina Paytan[1]**

[1]Earth and Planetary Sciences Department, University of Santa Cruz, Santa Cruz, California, USA, [2]Department of Earth System Science, University of California, Irvine, California, USA, [3]Department of Earth, Atmospheric and Planetary Sciences, Massachusetts Institute of Technology, Cambridge, Massachusetts, USA, [4]Department of Earth and Atmospheric Sciences, Cornell University, Ithaca, New York, USA, [5]Rosenstiel School of Marine and Atmospheric Science, University of Miami, Miami, Florida, USA

**Abstract** Bioassay incubation experiments conducted with nutrients and local atmospheric aerosol amendments indicate that phosphorus (P) availability limited phytoplankton growth in the low-nutrient low-chlorophyll (LNLC) ocean off Barbados. Atmospheric deposition provides a relatively large influx of new nutrients and trace metals to the surface ocean in this region in comparison to other nutrient sources. However, the impact on native phytoplankton is muted due to the high ratio of nitrogen (N) to P ($NO_3$:SRP $> 40$) and the low P solubility of these aerosols. Atmospheric deposition induces P limitation in this LNLC region by adding more N and iron (Fe) relative to P. This favors the growth of *Prochlorococcus*, a genus characterized by low P requirements and highly efficient P acquisition mechanisms. A global three-dimensional marine ecosystem model that includes species-specific phytoplankton elemental quotas/stoichiometry and the atmospheric deposition of N, P, and Fe supports this conclusion. Future increases in aerosol N loading may therefore influence phytoplankton community structure in other LNLC areas, thereby affecting the biological pump and associated carbon sequestration.

## 1. Introduction

Atmospheric deposition is a source of new N, P, and trace metals to the ocean [*Duce et al*., 1991, 2008; *Jickells et al*., 2005; *Kanakidou et al*., 2012; *Prospero et al*., 1996]. Nutrient inputs from atmospheric deposition have been shown to induce phytoplankton growth [*Boyd et al*., 1998; *Duarte et al*., 2006; *Erickson et al*., 2003], enhance N fixation at some oceanic locations [*Mills et al*., 2004], impact phytoplankton species dynamics [*Guo et al*., 2012; *Jordi et al*., 2012; *Mackey et al*., 2012b; *Paytan et al*., 2009], and intensify carbon sequestration via the biological pump [*Bressac et al*., 2014; *Guieu et al*., 2014b; *Krishnamurthy et al*., 2010; *Parekh et al*., 2006]. Atmospheric deposition of nutrients to the open oligotrophic ocean is particularly important in regions where there is little input from other new nutrient sources such as riverine input, ground water discharge, and sediment resuspension [*Jickells et al*., 2005]. The bioavailability of nutrients and trace metals from aerosols is directly related to the solubility of these components. Solubility is controlled by aerosol mineral compositions and the physical and chemical characteristics of the aerosol, as well as chemical transformations in the atmosphere during transport [*Anderson et al*., 2010; *Baker et al*., 2006b; *Hodge et al*., 1978; *Krishnamurthy et al*., 2009; *Mackey et al*., 2015a, 2012a; *Sedwick et al*., 2007]. Arid regions of North Africa are the most important mineral dust source to the North Atlantic [*Bristow et al*., 2010; *Husar et al*., 1997; *Schulz et al*., 2012]. The solubility of nutrients and trace metals from North African mineral dust is relatively low [*Sholkovitz et al*., 2012], and it increases only slightly after long-distance transport [*Baker et al*., 2006a].

Low availability of macronutrients (N, P) and metal micronutrients (Fe, Co) can limit or colimit phytoplankton growth in the ocean [*Morel et al*., 1994; *Saito et al*., 2008; *Sunda and Huntsman*, 1997] and drive genetic adaptation in different environments [*Mackey et al*., 2015b; *Morris et al*., 2012]. In contrast, high concentrations of some metals (e.g., Cu) can be toxic to phytoplankton [*Jordi et al*., 2012; *Mann et al*., 2002; *Paytan et al*., 2009; *Sunda and Huntsman*, 1992]. The supply of new nutrients to the surface ocean from atmospheric deposition has been determined by direct measurements and through modeling [*Baker et al*., 2003, 2010; *Boyd et al*., 2010; *Krishnamurthy et al*., 2010]. The impacts of atmospheric macro- and micronutrient deposition to the ocean have also been studied, particularly with respect to the impacts in iron-limited, high-nutrient

low-chlorophyll (HNLC) areas [*Bishop et al*., 2002; *Boyd et al*., 1998; *Jickells et al*., 2005]. Less work has been done to assess the impacts of deposition in the vast low-nutrient low-chlorophyll (LNLC) regions, which cover ~60% of the global ocean [*Giovagnetti et al*., 2013; *Mackey et al*., 2012b; *Paytan et al*., 2009; *Guieu et al*., 2014b].

Barbados is a tropical island located at the eastern edge of the oligotrophic Caribbean Sea. The open water primary producers in this region are dominated by small cells, with about 50% of the pigmented biomass contributed by picophytoplankton [*Dandonneau et al*., 2004]. *Prochlorococcus* is the most abundant photosynthetic organism in this environment, while picoeukaryotes and *Synechococcus* cell numbers are usually less than one tenth of *Prochlorococcus* [*Dandonneau et al*., 2004]. Large amounts of African dust are deposited in the Caribbean Sea around Barbados throughout the year, with the lowest deposition rates in winter and peak rates in the summer [*Trapp et al*., 2010]. Barbados receives relatively little anthropogenic air pollution from North America when compared to other subtropical islands such as Bermuda [*Savoie et al*., 2002]. Accordingly, the open water around Barbados is an excellent location for studying how African dust impacts phytoplankton growth and community dynamics in an oligotrophic LNLC setting.

Understanding how distinct phytoplankton species respond to nutrient loading from atmospheric deposition in Barbados can provide information on the impact of dust deposition on phytoplankton communities in other LNLC areas of the ocean. This is critical not only for our understanding of the current functioning of LNLC regions and the role these regions play in the carbon cycle but also for the projection of future changes, since significant changes in the magnitude of dust distribution [*Ginoux et al*., 2012; *Mahowald et al*., 2007; *Mahowald et al*., 2010; *Ward et al*., 2014] and future expansion of LNLC regions are predicted [*Henson et al*., 2010; *Steinacher et al*., 2010]. In this study we carried out bioassay incubations with locally collected aerosols and native phytoplankton assemblages collected offshore of Barbados to investigate the impact of atmospheric nutrient and trace metal inputs on phytoplankton productivity and community structure. We additionally employed a numerical model to explore how species-specific differences in phytoplankton cellular elemental ratios and regional variation in atmospheric deposition together influence phytoplankton community structure.

## 2. Observational Material and Methods

### 2.1. Aerosol Sample Collection and Analysis

Daily high-volume total suspended particles (TSP) filter samples were collected at Ragged Point on the easternmost coast of Barbados [*Trapp et al*., 2010; *Zamora et al*., 2013]. The TSP sampler operated only when winds were from the ocean sector to minimize local sources. Several filters collected between November 2009 and August 2010 were selected for the bioassay incubation experiments. Specifically, three sample sets were used in this study representing three seasons; winter, spring, and summer (Table 1). For the winter and summer two filters were combined to supply sufficient material for the experiment. These seasons capture differences in aerosol loading, chemical composition, and source, as described in previous studies from this region [*Yu et al*., 2015; *Jung et al*., 2013; *Prospero et al*., 2014]; however, the differences in the concentration of leachable nutrients and trace metals in the specific samples used were relatively small (see Table 1).

To determine the soluble nutrients and trace metal content of these samples, the filters were extracted by shaking for 1 h in Milli-Q water. The solution was then filtered (0.2 μm polysulfone membrane) and the soluble nutrients and trace metals in the filtrate were measured as described in *Chen et al*. [2006, 2007] (see Table 1).

### 2.2. Incubation Setup

Nutrient and aerosol addition bioassay experiments were carried out over 3 days in February 2012, similar to previous work by *Paytan et al*. [2009] and *Mackey et al*. [2012a, 2012b]. Surface seawater was collected from offshore (bottom depth >700 m) outside the Bellairs Research Institute at West Barbados (13°11.309′N, 59°38.267′W). Surface water was pumped into acid-cleaned sample-rinsed carboys using a peristaltic pump with acid-washed Teflon tubing and prefiltered through a 20 μm acid-washed Nitex© mesh to remove grazers. The seawater was stored in the dark during transport to the lab (<2 h). Seawater was dispensed into acid-washed and sample-rinsed polycarbonate bottles (500 mL each) and randomly assigned to different treatments (12–20 bottles per treatment). Treatments included single nutrient (N, P, or Fe) additions, as well

**Table 1.** Nutrients and Trace Metal Concentration is Aerosols Used for the Incubation Experiment and in the Bioassays at t0[a]

| Aerosol | Collection Dates | Atmospheric Dust Load | Weight on Filter | $NO_2 + NO_3$ | $NH_4$[b] | $PO_4$ | $NO_2 + NO_3$:P | Mn | Fe | Co | Ni | Cu | Cd | Pb |
|---|---|---|---|---|---|---|---|---|---|---|---|---|---|---|
| | | ($\mu g\ m^{-3}$) | ($mg\ cm^{-2}$) | Soluble Fraction ($nmol\ mg^{-1}$) | | | | | | | | | | |
| 1 | 11/25/2009 to 11/27/2009 | 33.9 | 0.0796 | 164 | 182 | 2.6 | 64 | 4.1 | 1.08 | 0.032 | 0.09 | 0.14 | 0.0025 | 0.0003 |
| 2 | 3/31/2010 to 4/1/2010 | 91.6 | 0.1546 | 231 | 256 | 5.4 | 43 | 4.2 | 0.31 | 0.015 | 0.03 | 0.05 | 0.0008 | 0.0001 |
| 3 | 8/17/2009 to 8/19/2009 | 14.8 | 0.0902 | 357 | 395 | 2.7 | 132 | 2.5 | 0.28 | 0.013 | 0.05 | 0.09 | 0.0007 | 0.0001 |
| | | | | *Bulk Composition ($nmol\ mg^{-1}$)* | | | | | | | | | | |
| 1 | 11/25/2009 to 11/27/2009 | | | | | 27.8 | | 10.1 | 619 | 0.228 | 0.24 | 0.68 | 0.003 | 0.12 |
| 2 | 3/31/2010 to 4/1/2010 | | | | | 37.0 | | 17.0 | 913 | 0.350 | 0.96 | 0.58 | 0.006 | 0.16 |
| 3 | 8/17/2009 to 8/19/2009 | | | | | 34.6 | | 12.5 | 899 | 0.342 | 0.66 | 0.79 | 0.004 | 0.19 |
| | | | | *% Solubility* | | | | | | | | | | |
| 1 | 11/25/2009 to 11/27/2009 | | | | | 9.3 | | 40.5 | 0.17 | 14.0 | 36.9 | 20.7 | 96 | 0.25 |
| 2 | 3/31/2010 to 4/1/2010 | | | | | 14.6 | | 24.7 | 0.03 | 4.3 | 3.1 | 8.6 | 13 | 0.06 |
| 3 | 8/17/2009 to 8/19/2009 | | | | | 7.8 | | 20.0 | 0.03 | 3.8 | 7.6 | 11.4 | 16 | 0.05 |
| Amendments | | | | *Concentrations in Amended Seawater at t0 ($nmol\ kg^{-1}$)* | | | | | | | | | | |
| Control | | | | 330 | 305 | BD | >27.5[c] | 2.87 | 1.02 | 0.01 | 2.00 | 2.19 | 0.06 | 0.04 |
| NO3 + NH4 | | | | 11107 | 805 | 17 | 647 | 2.81 | 0.91 | 0.004 | 1.88 | 2.14 | 0.06 | 0.04 |
| PO4 | | | | 288 | 305 | 490 | 0.59 | 2.32 | 1.42 | 0.009 | 2.04 | 2.26 | 0.07 | 0.05 |
| NO3 + NH4 + PO4 | | | | 11111 | 609 | 506 | 21.9 | 2.04 | 0.81 | 0.004 | 1.71 | 2.29 | 0.05 | 0.05 |
| Fe + NO3 + NH4 | | | | 9839 | 657 | BD | >820[c] | 2.49 | 8.48 | 0.010 | 1.83 | 2.78 | 0.06 | 0.05 |
| Spring dust low | | | | 251 | 241 | BD | >21.0[c] | 3.41 | 0.89 | 0.010 | 1.94 | 2.23 | 0.06 | 0.05 |
| Spring dust high | | | | 689 | 578 | 27 | 25.4 | 9.97 | 1.00 | 0.033 | 1.68 | 2.46 | 0.06 | 0.05 |
| Summer dust low | | | | 407 | 274 | BD | >33.9[c] | 2.98 | 0.47 | 0.013 | 1.67 | 2.15 | 0.05 | 0.05 |
| Summer dust high | | | | 457 | 682 | 17 | 27.6 | 8.13 | 1.15 | 0.033 | 1.97 | 2.16 | 0.07 | 0.06 |
| Winter dust high | | | | 442 | 425 | 19 | 23.7 | 8.89 | 1.54 | 0.052 | 1.98 | 2.24 | 0.06 | 0.04 |

[a]BD, below detection limit. Aerosol 1 (winter) has slightly higher trace metals compared to 2 and 3. Aerosol 2 (spring) slightly higher P. Aerosol 3 (summer) lower Mn. Dates are formatted as month/day/year.
[b]Dust $NH_4$ were calculated by multiplying N + N by average $NH_4$ to N + N ratio in Barbados dust described in *Zamora et al.* [2011].
[c]Estimated by using detection limit of $PO_4$ as the upper limit of $PO_4$ concentration.

as a combination of N and P and a combination of N and Fe, at concentrations representative of deep water in this area (see Table 2). The selected aerosol samples representing the three seasons (described above) were immersed in 50 mL of locally collected seawater (the same water used for the incubation experiment), shaken for 1 h and filtered through a 0.2 μm polysulfone membrane syringe filter. The seawater containing the

**Table 2.** Amendments to Incubation Bottles

| Treatment | Concentration |
|---|---|
| Control | No addition |
| $NO_3 + NH_4$ | Deep water (200 m) concentration, 10 μM $NO_3$ and 0.5 μM $NH_4$ |
| $PO_4$ | Deep water (200 m) concentration, 0.5 μM $PO_4$ |
| $NO_3 + NH_4 + PO_4$ | As above |
| African dust, low | 0.03 mg dust per 500 mL water |
| African dust, high | 0.5 mg dust per 500 mL water |
| $Fe + NO_3 + NH_4$ | Fe 10 nmol/kg (10 times the ambient seawater concentration of ~1 nmol/kg) 10 μM $NO_3$ and 0.5 μM $NH_4$ |

soluble fraction of the aerosols was added to the incubation bottles in volumes that represent aerosol loads during "typical" and "high" deposition events in this region (Table 2 and see also supporting information). High and low deposition rates used for the additions were calculated based on atmospheric deposition estimates from *Mahowald et al*. [2005]; the "typical" deposition corresponds to annual average dust deposition rates in Barbados during summer, ~10 g $m^{-2}$ $yr^{-1}$, and the high deposition represents extreme dust storms corresponding to a fifteenfold increase in deposition, ~150 g $m^{-2}$ $yr^{-1}$ [*Jung et al*., 2013]. The amount of dust added simulates the cumulative deposition flux over 20 days to the upper 10 m mixed layer. Details for the calculation of the amount of dust added are provided in the supporting information. Concentrations of nutrients and metals at the start of the incubations, immediately after the amendments were added, are reported in Table 1. A control (no addition, blank filter extract) treatment and procedural blanks (Milli-Q water) were also included. All bottles were incubated in a pool filled with circulating seawater to maintain the local surface ocean temperature. The pool was covered with a neutral density shading screen to reduce light intensity by 50% [*Mackey et al*., 2012b]. Water samples used for the experiment (preadditions) were collected to characterize the baseline seawater chemistry (five replicates) and three replicate bottles for each treatment were collected immediately after the additions were administered (time zero, t0). The experiment took place over a total of 3 days. Each day at 4 pm, three bottles were randomly selected from each nutrient treatment, while five bottles were randomly selected from each aerosol treatment (e.g., time points t1–t3). Immediately upon collection, each bottle was sampled for chlorophyll *a* (Chl *a*), flow cytometry, nutrients, and trace metal concentrations (see below).

Statistical significance was tested with one-way analysis of variance (ANOVA) to check for differences between the mean values, and Dunnett's test was then applied to compare control values with other treatments.

### 2.3. Nutrient Analyses

Soluble nutrients from the direct extraction of aerosol samples were analyzed on a flow injection autoanalyzer (FIA, Lachat Instruments model QuickChem 8000). Detection limits for soluble reactive phosphorus (SRP) and nitrate plus nitrite (N + N) were 0.1 μM and 0.29 μM. Ammonium ($NH_4^+$) concentrations were calculated according to the average $NH_4^+$ to N + N ratio in dry deposition samples for the region as described in *Zamora et al*. [2011].

Seawater from each of the retrieved incubation bottles was filtered through a sample-rinsed 0.2 μm filter (Polyethersulfone, 150 ml Bottle Top Filter, CORNING), collected in acid-washed 50 mL falcon tubes and frozen until nutrients were analyzed. SRP and $NH_4^+$ were measured by a continuous flow autoanalyzer (TechniconAutoAnalyzer II™). SRP measurements followed a modification of the molybdenum blue procedure [*Bernhardt and Wilhelms*, 1967] and $NH_4^+$ analysis was done using a method modified from ALPKEM RFA methodology. N + N was analyzed by Alpkem RFA 300 following methods from *Armstrong et al*. [1967]. Detection limits for SRP, N + N, and $NH_4^+$ were 0.012 μM, 0.03 μM, and 0.05 μM, respectively. Our estimates of the detection limits are based on 3 times the lowest resolvable signal from the instrument.

### 2.4. Trace Metals Analysis

For trace metal analyses 60 mL subsamples of 0.2 μm filtered water were collected in acid-washed, sample-rinsed LDPE bottles. Seawater samples were acidified to pH $< 2.0$ by adding 45 μL of concentrated trace metal grade $HNO_3$ at least 24 h prior to column chemistry. Nobias Chelate-PA1 resin (HITACHI, Japan) was used for seawater matrix removal and trace metal preconcentration [*Biller and Bruland*, 2012; *Sohrin et al*., 2008]. Recovery yields are summarized in Table S1 of the supporting information. A 5 mL eluent from each sample was analyzed for a suite of trace metals (Mn, Fe, Co, Ni, Cu, Cd, and Pb) by HR-ICPMS (Thermo Element XR). Samples were introduced into the instrument with a peristaltic pump at a flow rate of ~120 μL $min^{-1}$ and passed through an ESI-PC3 Peltier cooled spray chamber before entering the torch. Sample and gas flow rates were optimized for each run; values were 0.75–0.80 ml $min^{-1}$ and 0.20–0.24 ml $min^{-1}$, respectively. In, Y, and Sc were added to each sample as internal standards for calibrating sensitivity shifts of the instrument. Method accuracy and precision were assessed relative to Certified Reference Material CASS5 and GEOTRACES SAFe reference seawater (Table S1).

### 2.5. Chlorophyll *a* Concentration and Flow Cytometry

From each bottle, 100 mL of seawater was filtered onto GFF filters, which were frozen in liquid nitrogen and then stored at −80°C until analyzed. Upon return from the field, samples were extracted for 24 h in the dark at

−20°C in 90% acetone. Fluorescence was measured on a TD-700 fluorometer (Turner Designs) calibrated with fresh Chl *a* standard from *Anacystis nidulans* (Sigma).

Water samples (1.5 mL) were collected from each incubation bottle for flow cytometry, preserved by adding 300 μL of formalin, frozen in liquid nitrogen, and stored at −80°C until analysis. Approximately 10,000 beads 0.75 μm in diameter (Fluoresbrite™ particles, YG, Polysciences, Inc.) were added to each sample, and samples were analyzed by flow cytometer (BD Influx cell sorter) triggering on forward angle light scatter (FSC). Total cell concentrations of *Prochlorococcus*, *Synechococcus*, and picoeukaryotic were enumerated. The groups were differentiated based on their characteristic autofluorescence and scattering properties (Figure S1 in the supporting information).

## 3. Numerical Modeling

The contribution of soluble nutrients from atmospheric deposition (based on a deposition model, see below) relative to other sources of nutrients to the surface mixed layer (based on an ocean-ecosystem model) was derived. The resulting impact on phytoplankton dynamics and species distribution was assessed in order to test if results from the incubation bioassays can be reproduced in silico at the location of the experiment. These new model simulations are unique, as we incorporate atmospheric deposition of multiple nutrients, internal cycling of nutrients in the ocean, and taxa-specific quotas for nutrient uptake.

### 3.1. Atmospheric Deposition Model

Simulations of N, P, and Fe deposition were conducted using the Community Atmospheric Model (CAM4), and online (climate model derived) winds with the slab ocean model [*Neale et al*., 2013]. Simulations were conducted for 5 years, with the last year used for analysis. By using the prescribed aerosols for radiative transfer calculations, the meteorology in all the simulations was identical. The model simulates three-dimensional transport and wet and dry deposition for gases and aerosols [*Lamarque et al*., 2011; *Mahowald et al*., 2006; *Rasch et al*., 2000]. For N, the CAM-chem model was used [*Lamarque et al*., 2011], which simulates tropospheric chemistry, including ozone and organic compounds for current and preindustrial emissions using the emission data sets from *Lamarque et al*. [2010], except for fires. The baseline fire emissions used are the observation-based Global Fire Emission Database version 3 (GFED3) [*Randerson et al*., 2013; *van der Werf et al*., 2006]. We use the tuning methodology of *Ward et al*. [2012] in which, briefly, GFED fire emissions are scaled to ground and space-based observations of aerosol optical depth (AOD) for 14 regions by identifying high-fire emission and low-fire emission months for each region. The tuning factors are applied to all the species emitted by fire, including N, Fe, and P species. P was modeled following *Mahowald et al*. [2008] with some small differences (see supporting information). Fe is modeled following *Luo et al*. [2008]. Dust is assumed to contain 3.5% Fe, the same as average crustal abundance [*Hans Wedepohl*, 1995] and as previously measured on samples from this site [*Trapp et al*., 2010]. Biomass burning is assumed to have a ratio of 0.2 gFe/g black carbon (BC) in the fine mode, and 1.4 gFe/gBC for the coarse mode [*Luo et al*., 2008]. Industrial sources of Fe are emitted following *Luo et al*. [2008]. Source specific solubility was applied to the various P and Fe sources as discussed in the supporting information. The model output also produces the N:P ratio of the soluble fraction of atmospheric deposition to the ocean, which is as previously reported much higher than the Redfield Ratio (16N:1P) throughout the ocean [*Okin et al*., 2011]. More detail on the deposition model is provided in the supporting information. Model-derived atmospheric deposition and associated nutrient and Fe input fluxes, along with dust, nutrient, and trace metal concentrations from the bioassay experiments are listed in Table 3.

### 3.2. Ocean Model

To investigate the implication of the high N:P ratio dust deposition on marine phytoplankton, and particularly to highlight the unique setting of our study region compared to the rest of the ocean, we employed a global three-dimensional model that includes physical, biogeochemical, ecosystem, and radiative transfer components, as well as an atmospheric deposition component [*Dutkiewicz et al*., 2015]. The biogeochemical/ecosystem model resolves the cycling of C, P, N, silica (Si), Fe, and oxygen (O) through inorganic, living, dissolved, and particulate organic phases. The biogeochemical and biological tracers are transported and mixed using the MIT general circulation model (MITgcm) [*Marshall et al*., 1997], which is constrained to be consistent with altimetric and hydrographic observations (the ECCO-GODAE state estimates, [*Wunsch and Heimbach*, 2007]). This configuration has a

**Table 3.** Model-Derived Atmospheric Deposition and Associated Nutrients and Iron Input Fluxes and Dust, Nutrients and Trace Metals Added in the Bioassay Experiments

| | Dust Flux | Dust Addition | N | $PO_4$ | Fe |
|---|---|---|---|---|---|
| | ($gm^{-2}\ yr^{-1}$) | ($mg\ L^{-1}$) | | ($mmol\ m^{-2}\ yr^{-1}$) | |
| Mode annual average | 8.7 | NA | 7.5 | 0.019 | 0.044 |
| | | | | ($nmol\ L^{-1}$) | |
| Dust bioassay low | 10 | 0.06 | 31.7 | 0.213 | 0.034 |
| Dust bioassay high | 150 | 1 | 528 | 3.55 | 0.56 |

1° × 1° horizontal resolution and 23 vertical levels ranging from 10 m in the surface ocean to 500 m at depth. We resolve two grazers and phytoplankton analogues of *Prochlorococcus*, *Synechococcus*, picoeukaryotes, coccolithophores, diatoms, and nitrogen fixing diazotrophs. The phytoplankton types differ in their growth parameters, nutrient requirements, as well as their pigment compositions. The biogeochemical and biological tracers interact through the formation, transformation, and remineralization of organic matter. Excretion and mortality transfer living organic material into sinking particulate and dissolved organic detritus, which are respired back to inorganic forms. Fe chemistry includes complexation and scavenging by particles [*Parekh et al*., 2005], as well as sedimentary sources following *Elrod et al*. [2004]. Full equations and parameter values are provided in *Dutkiewicz et al*. [2015].

In the original model [*Dutkiewicz et al*., 2015] the only element included in the atmospheric nutrient deposition was Fe. Here we incorporated additional deposition of $PO_4^{3-}$, $NO_y$ ($NO_3^-$ and other oxidized N species) and $NH_4^+$ along with Fe as provided by the deposition model described in section 3.2. We also introduced a crude representation of sedimentation as a constant rate of POM reaching the sea floor.

In the original model [*Dutkiewicz et al*., 2015] all phytoplankton types, except diazotrophs, had the same C:N:P:Fe stoichiometric ratios. Because a central hypothesis of this study is that species-specific differences in elemental ratios are important for determining nutrient limitation status in this region (i.e., as observed in the incubation experiments), we also altered the model such that the stoichiometry of each phytoplankton functional group reflects literature values of C:N:P (Table S2). In particular, *Prochlorococcus* has a high N:P ratio (25:1), while *Synechococcus* has a lower N:P ratio (21:1), though still higher than picoeukaryotes (15:1).

Initial conditions use macronutrient fields ($NO_3^-$, $PO_4^{3-}$ and silicic acid) from the World Ocean Atlas climatology [*Garcia et al*., 2006], and the Fe, $NH_4^+$, nitrite, dissolved and particulate matter from previous simulations [*Dutkiewicz et al*., 2015]. The plankton biomass is also initialized from previous model output, divided equally between groups. We ran the simulation forward for 10 years with a repeating generic "year" from the physical ECCO-GODAE products [*Wunsch and Heimbach*, 2007]. The phytoplankton establish a repeating pattern after about 3 years. A slow drift as deep water nutrient distributions adjust does not significantly change the results over the remaining time period. We show results from two simulations: (1) EXP1, where the elemental stoichiometry was the same between all phytoplankton (except diazotrophs) as in *Dutkiewicz et al*. [2015] and (2) EXP2, where the phytoplankton types had differing stoichiometry as discussed above (Table S2). We show the difference between the 10th year of each simulation.

In order to investigate the relative contribution of nutrients from different sources in the Atlantic Ocean, we used the model to calculate the relative contribution of N and P from atmospheric deposition to other nutrient inputs, including lateral advection, vertical advection and diffusion, and remineralization of dissolved organic matter (Figure 4).

## 4. Results

### 4.1. Aerosol Soluble Nutrient and Trace Metal Concentrations

Seawater soluble nutrients and select trace metal concentrations of the aerosol samples used in the bioassay incubation experiments are shown in Table 1. Aerosol 1 (winter) has slightly higher levels of soluble trace metals compared to aerosol samples 2 (spring) and 3 (summer). Aerosol sample 2 has slightly higher P concentration (5.4 $nmol\ mg^{-1}$) than aerosol samples 1 (2.6 $nmol\ mg^{-1}$) and 3 (2.7 $nmol\ mg^{-1}$). Aerosol 3 has higher N + N and lower Mn compared to aerosols 1 and 2. Overall the differences in the soluble fraction of nutrients and trace metals between these seasonally distinct aerosol samples were small (less than an order

**Table 4.** Nutrient and Trace Metal Concentrations in Baseline Incubation Seawater

| Nutrients | Baseline Seawater (μM) (Mean ± SE[d]) | Caribbean/Tropical Atlantic Seawater |
|---|---|---|
| $PO_4$ | BD | 0.04–0.14[a] |
| N + N | 0.241 ± 0.098 | 0–0.94[a] |
| $NH_4$ | 0.228 ± 0.093 | |
| N + N:P | >20[e] | 0–19.2 |
| $NO_3 + NH_4$:P | >39[e] | |
| Trace metals | (nmol/kg) | |
| Pb | 0.066 ± 0.016 | 0.01[b] |
| Cd | 0.048 ± 0.026 | 0.0005[b] |
| Mn | 2.4 ± 0.115 | 3.19[b] |
| Fe | 1.09 ± 0.264 | 0.53[b], 1.31[c] |
| Co | 0.032 ± 0.012 | |
| Ni | 1.8 ± 0.078 | 2.16[b] |
| Cu | 2.3 ± 0.203 | |

[a]Data from World Ocean Database, nitrogen contains only nitrate value.
[b]From GEOTRACES GA02 cruise station 33 (same latitude).
[c]*Fitzsimmons et al.* [2013].
[d]Standard error.
[e]Estimated by using the detection limit of $PO_4$ as the upper limit of $PO_4$ concentration.

of magnitude). The bulk composition of dust samples was analyzed following a strong acid ($HNO_3$ and HF) digestion [*Morton et al.*, 2013]. The solubility of P was higher in sample 2 (spring) and ranged from 7.8% to 14.6% among the samples. Overall, trace metal solubility was higher in Aerosol 1 (winter; Table 1).

### 4.2. Baseline Seawater Chemistry

The seawater used for the experiments had low baseline nutrient concentrations and relatively high Fe (1.09 ± 0.264 nmol $kg^{-1}$). Mean baseline nutrient concentrations were 0.241 ± 0.098 μM for N + N and 0.228 ± 0.093 μM for $NH_4^+$, while SRP was below detection (<12 nM). Trace metal levels were in the same range as previously published data for this region [*Fitzsimmons et al.*, 2013; *Mawji et al.*, 2015; *Rijkenberg et al.*, 2014]. Concentration levels and ratios between nutrients are shown in Table 4 along with previously reported surface seawater concentrations for this region.

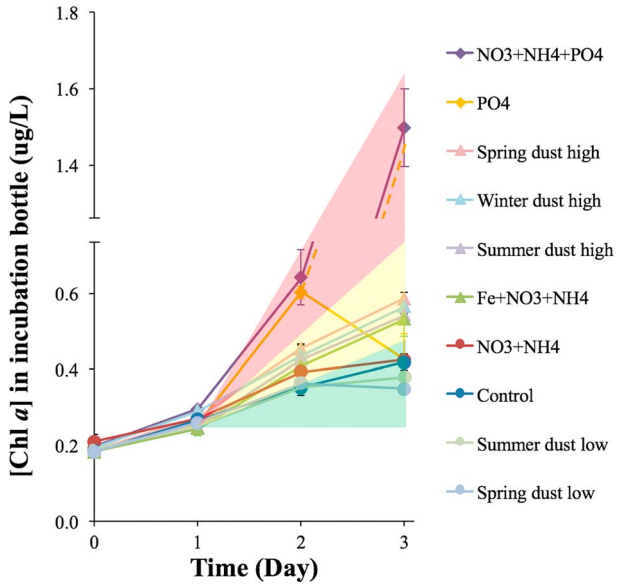


**Figure 1.** Growth response of phytoplankton under different nutrient addition during three consecutive days. Dashed line at phosphate represents expected response of phytoplankton growth without nitrogen limitation. Note break in scale for Chl *a*.

### 4.3. Chlorophyll *a*

Chlorophyll *a* (Chl *a*) concentration in the seawater sample collected for the experiment (baseline) was 0.19 ± 0.01 (average ± SE) mg $m^{-3}$. After 3 days of incubation Chl *a* increased twofold to 0.42 ± 0.02 mg $m^{-3}$ in the control bottles. Similar increases in Chl *a* were observed at day 3 for the addition of N alone and for all dust additions (Figure 1), though not significantly different than the control at $p < 0.05$. After 3 days of incubation, Chl *a* in the Fe + N and the high dust additions for all 3 seasons (Spring high, Summer high, and Winter high) were 0.53 ± 0.05, 0.59 ± 0.02, 0.54 ± 0.02, and 0.57 ± 0.02 mg $m^{-3}$, respectively. This was an approximately threefold increase compared to t0 and was higher than the control values at day 3. The increases compared to those of the control are statistically significant

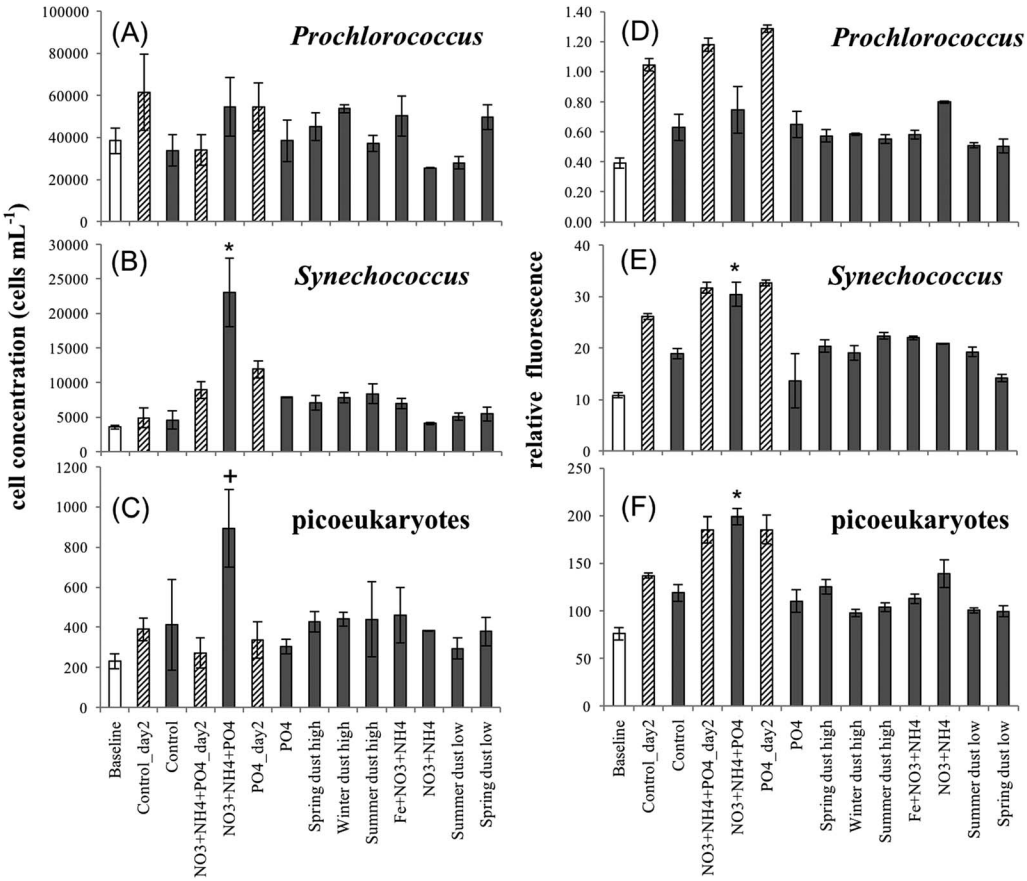


**Figure 2.** Growth response of phytoplankton on day 3, control, N + P and $PO_4$ are also reported for day 2. Cell concentrations of (a) *Prochlorococcus*, (b) *Synechococcus*, and (c) picoeukaryotes on day 3 (cell $ml^{-1}$). Relative phytoplankton fluorescence of (d) *Prochlorococcus*, (e) *Synechococcus*, and (f) picoeukaryotes were normalized with 0.75 μm beads' fluorescence. Note that significance was not determined for the P day 2 treatment as it is not comparable to the other data which use day 3 results; however, day 2 P is significantly different than day 2 control in fluorescence (day 2 data shown in striped bars). Growth condition that were statistically different from the control incubation water at day 3 are marked as "asterisk" for $P < 0.05$ and "cross" for $P = 0.104$.

for Spring high and Winter high ($p = 0.011$, 0.034). Chl *a* in the N + P treatment showed the largest and most pronounced change, increasing eightfold compared to the baseline level from 0.19 to $1.50 \pm 0.10$ mg $m^{-3}$. This increase is significantly different than the Chl *a* increase in the control after 3 days of incubation ($p = 0.00001$). Chl *a* increased at the same rate in the P alone addition for the first 2 days of incubation (0.6 mg $m^{-3}$ on day 2 increasing threefold compared to the baseline); however, in day 3 the levels decreased sharply and were similar to those of the control at the end of the experiment (Figure 1).

### 4.4. Phytoplankton Abundance

Cell abundances of *Prochlorococcus*, *Synechococcus*, and picoeukaryotes changed over time in the treatments (Figures 2a–2c). The most abundant species in the baseline water sample was *Prochlorococcus* with $38.4 \pm 6.1 \times 10^3$ cells $mL^{-1}$ (91% of cells), followed by *Synechococcus* with an order of magnitude fewer cells ($3.6 \pm 0.3 \times 10^3$ cells $mL^{-1}$, 8.5% of cells) and picoeukaryotes comprising only ~0.05% of cells ($0.23 \pm 0.04 \times 10^3$ cells $mL^{-1}$). After 3 days of incubation, increases in *Synechococcus* and picoeukaryotes abundance were more pronounced compared to those of *Prochlorococcus* in all treatments that show a response in Chl *a* (e.g., high dust and N + P). In the N + P treatment, cell numbers of *Synechococcus* and picoeukaryotes increased fivefold to $23.1 \pm 5.0 \times 10^3$ cells $mL^{-1}$ and $0.9 \pm 0.2 \times 10^3$ cells $mL^{-1}$, respectively. Although *Prochlorococcus* still comprised the largest fraction of the population (70%) they increased to a lesser extent (only 42% to $54.4 \pm 13.9 \times 10^3$ cells $mL^{-1}$). After 3 days of incubation the *Synechococcus* and picoeukaryotes cell number in the Fe and high dust additions also increased but only by a factor of 2 compared to the

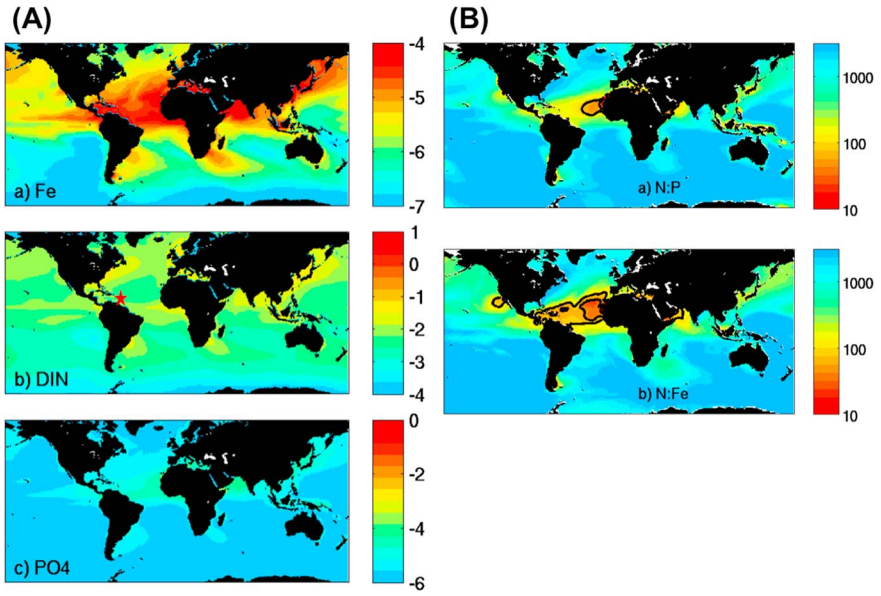


**Figure 3.** (A) Bio-available aeolian deposition of (a) Fe (mol Fe $m^{-2}$ $y^{-1}$), (b) $NO_3 + NO_2 + NH_4$ (mol N $m^{-2}$ $y^{-1}$), (c) $PO_4$ (mol P $m^{-2}$ $y^{-1}$), values are in log scale. Red star in Figure 3b represents for dust sampling site. (B) Ratio of aeolian deposition: (a) $(NO_3 + NO_2 + NH_4)$:$PO_4$ (mol N/mol P), (b) $(NO_3 + NO_2 + NH_4)$:Fe (mol N/mol Fe). With contours [40, 80] for N:P and [20, 50, 100] for N:Fe.

baseline ($7.1 \times 10^3$ to $8.4 \times 10^3$ cells $mL^{-1}$ and $0.43 \times 10^3$ to $0.46 \times 10^3$ cells $mL^{-1}$). Unlike *Synechococcus* and picoeukaryotes, cell levels of *Prochlorococcus* on day 3 in these treatments did not show a significant difference when compared with the control, with numbers varying from $25.5 \times 10^3$ cells $mL^{-1}$ to 54.4 cells $mL^{-1}$.

Fluorescence per cell values (normalized to 0.75 μm beads) in the control incubation at day 3 for *Prochlorococcus*, *Synechococcus*, and picoeukaryotes are 0.63, 18.92, and 119.05, respectively. In the N + P treatment, fluorescence per cell almost doubled in *Synechococcus* and picoeukaryotes (30.5 and 199), while the response was small in *Prochlorococcus* (0.75). Day 3 fluorescence values in the P treatment are close to those in the control (similar to Chl *a*), however, day 2 levels for *Synechococcus* and picoeukaryotes are 32.7 and 185.5, which are similar to those of the N + P treatment (31.7 and 185.2) (Figures 2d–2f).

Interestingly, the response observed in the dust amendments was limited to the high dust additions, and even that response was relatively small when compared to treatments where P was added. Specifically, addition of locally collected aerosols at rates similar to average deposition in this area did not trigger much growth of *Synechococcus*, picoeukaryotes, or *Prochlorococcus*, and even introduction at levels equivalent to those expected after 20 days of heavy dust storms resulted in a relatively small increase in Chl *a*, which is consistent with previous incubation experiments where high amounts of Saharan dust (2 mg $L^{-1}$) were added and the primary response measured was bacterial production [*Maranon et al.*, 2010]. This indicates that even extremely high levels of atmospheric deposition are not sufficient to completely alleviate the P limitation and induce substantial autotrophic growth in this region of the ocean.

### 4.5. Deposition Model

Annually averaged deposition maps of N, P, and Fe based on aerosol loads (dust and anthropogenic emissions) and specific solubility of each element, are shown in Figure 3A; a large spatial variability is simulated, consistent with observations e.g.. *Baker and Croot*, 2010; *Baker et al.*, 2010; *Dentener et al.*, 2006; *Mahowald et al.*, 2008, 2009; *Sholkovitz et al.*, 2012]. The N:P and N:Fe ratio based on these deposition fields are calculated and shown in Figure 3b. The ratio of N:P in the soluble fraction of aerosols (~50:1 to >1000:1; Figure 3b) is much higher than the ratio typically required by phytoplankton (16:1) [*Okin et al.*, 2011]. In particular, some of the highest N:P deposition ratios are found in the central North Atlantic subtropical gyre.

### 4.6. Ocean Model

Our ocean model shows that the N enrichment in dust and the high rates of deposition around the Caribbean, particularly around our sampling area, result in a relatively higher contribution of atmospheric N compared to

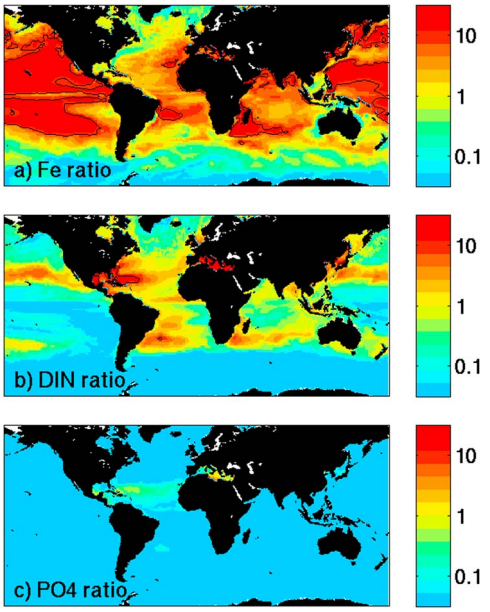


**Figure 4.** Relative contribution (%) of dust to the model-derived supply of nutrients to the top 100 m on the ocean for (a) Fe, (b) dissolved inorganic nitrogen (DIN), and (c) $PO_4$. The "in water" supplies include vertical and horizontal advection and diffusion, as well as remineralization of organic matter. Contour is 10%. Color bars are in log scale.

other sources of nutrients (advection, diffusion, and remineralization of organic matter) (Figure 4). This tends to shift the total nutrient input ratio to the surface waters in this region toward higher N:P ratio, and toward P limitation. This regional increase in the relative contribution of aerosol nutrients to the combined nutrient inputs in the surface layer is also consistent with calculations using upwelling found by *Oschlies and Garcon* [1998] (Table 5).

The phytoplankton community in the North Atlantic subtropical gyre is dominated by picophytoplankton (Figures 5a–5c) in both model experiments (and the original model [*Dutkiewicz et al.*, 2015]). However, there is a substantial difference (Figures 5d–5f) in the relative abundance of the three picophytoplankton groups between EXP1 (where species-specific elemental ratios were all the same except for *Trichodesmium*) and EXP2 (where species-specific elemental ratios were used). In particular, there is a significant difference in the region where the influence of atmospheric deposition with high N:P ratio is highest compared to other nutrient sources (upwelling, advection) (Figure 4). In this P-limited LNLC region, *Prochlorococcus* becomes more abundant when the model accounts for its low P requirements in EXP2 compared to EXP1. Specifically, with their lower P requirements as simulated in EXP2 relative to EXP1, *Prochlorococcus* biomass increases (see red box in Figure 5) in the region with the highest aerosol N:P ratios. On the other hand, neither *Synechococcus* nor picoeukaryotes, with their lower N:P requirements, have any benefit in this mostly oligotrophic and P-limited region. However, on the edge of the gyre, we find the opposite response. Here where N is limiting, the high N:P quota of *Prochlorococcus* is not beneficial and *Synechococcus* increases in biomass at the expense of *Prochlorococcus*.

The main result from the difference between the two simulations is that the combination of including N and P in addition to Fe for the atmospheric deposition and using taxa-specific nutrient elemental ratios results in significant changes in phytoplankton species distribution. Specifically, *Prochlorococcus*, with its low P

**Table 5.** Relative Contribution of Nutrient Sources in Each Region of Atlantic Ocean

| | Upwelling Fluxes (mmol $m^{-2}$ $yr^{-1}$) | | | Dust Fluxes (mmol $m^{-2}$ $yr^{-1}$)[d] | | Dust flux to upwelling | |
|---|---|---|---|---|---|---|---|
| | $NO_3$[b] | $NO_3$:$PO_4$[c] | $PO_4$ | N | $PO_4$ | N | P |
| Subpolar 50 N–65 N | 410 | 15.2 | 27.0 | 14.2 | 0.003 | 3.5% | 0.01% |
| Midlatitude 30 N–50 N | 580 | 20.0 | 29.0 | 17.7 | 0.006 | 3.5% | 0.02% |
| Subtropical gyre 12 N–30 N, 70 W–22 W | 47 | 25.4 | 1.85 | 6.2 | 0.017 | 13.1% | 0.9% |
| Tropical 8 S–8 N | 370 | 14.9 | 24.9 | 17.4 | 0.022 | 4.7% | 0.09% |
| Barbados (13.1 N, 59.5 W)[a] | 47 | 25.4 | 1.85 | 7.5 | 0.019 | 15.9% | 1.04% |

[a] N and P fluxes are from *Zamora et al.* [2013].
[b] $NO_3$ upwelling fluxes are from *Oschlies and Garcon* [1998, Table 1].
[c] N to P ratios are median value of N:P at depth 150 m from GEOTRACES cruise GA02.
[d] Dust fluxes are from model results described in this paper, values are average fluxes of different regions defined in *Oschlies and Garcon* [1998].

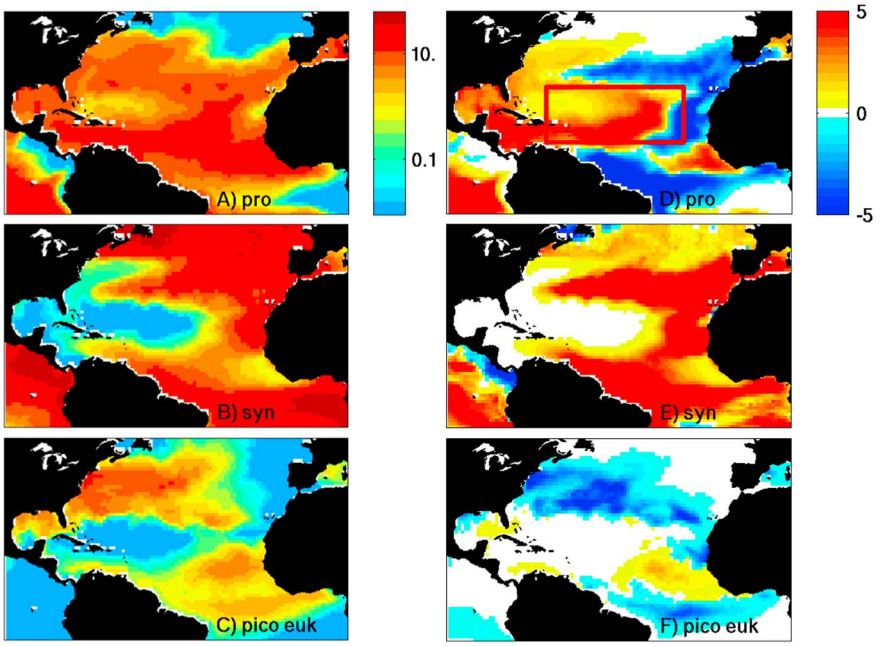


**Figure 5.** Biomass of phytoplankton in the top 10 m (mg C $m^{-3}$) in our model where phytoplankton have differing stoichiometry (EXP2): (a) *Prochlorococcus*, (b) *Synechococcus*, and (c) picoeukaryotes. Difference (mg C $m^{-3}$) between simulations where all phytoplankton have same stoichiometry (EXP1) and (EXP2): (d) *Prochlorococcus*, (e) *Synechococcus*, and (f) picoeukaryotes. Positive values indicate higher biomass in EXP2 when different phytoplankton stoichiometry is considered. *Prochlorococcus* biomass that was 5 mg C $m^{-3}$ higher in EXP2 than EXP1 was observed at our study site. (Note that our study site is located at the southwest part of the north Atlantic subtropical gyre, which is defined as the region between 12 N–30 N and 70 W–22 W.)

requirement relative to N (Table S2), thrive and become more prolific in the high N:P ratio regions, particularly in our study area.

## 5. Discussion

### 5.1. Nutrient Limitation in the Caribbean Sea

The Caribbean Sea comprises a significant fraction of the western North Atlantic Ocean and generally fluctuates little in its hydrographic conditions [*Mullerkarger et al*., 1988]. The area is characterized by relatively low productivity, low nutrients, and low chlorophyll levels [*Garcia et al*., 2010]. Previous studies, primarily from HNLC areas of the ocean, show that low atmospheric deposition rates and low Fe availability limit ocean productivity [*Bishop et al*., 2002; *Boyd et al*., 1998; *Erickson et al*., 2003; *Jickells et al*., 2005]. However, the role atmospheric deposition plays in influencing phytoplankton dynamics in LNLC regions has only recently begun to receive more attention [*Giovagnetti et al*., 2013; *Guieu et al*., 2014a; *Mackey et al*., 2012b; *Paytan et al*., 2009; *Wuttig et al*., 2013]. Specifically, deposition rates are high in the Barbados region, yet LNLC conditions persist. High deposition rates are expected to supply new nutrients and sustain relatively high levels of productivity downwind of high deposition areas, yet productivity and Chl *a* concentrations in the euphotic zone of the LNLC-high dust deposition areas in general, and at our study site off Barbados in particular, are relatively low (Figure 5) [*Volpe et al*., 2009].

To understand this observation, it is important to determine what limits productivity in the surface waters of the Caribbean Sea, as well as the role nutrients supplied from aerosol deposition play in such systems. In our incubation experiments, N addition (as a mixture of $NO_3^-$ and $NH_4^+$) induced minimal response in Chl *a* or species abundance relative to the control, suggesting that N was not the limiting nutrient in the water at the time our samples were collected. The largest Chl *a* increase was obtained with treatments that received P addition as N + P or P alone (during the first 2 days), indicating that P was limiting growth in this region during our experiment (Figure 1). Indeed, measurable net P drawdown, calculated by the difference in SRP concentrations between t0 and t3, was only seen in the treatments that received P additions (Figure S2); N

drawdown was also seen in these treatments, consistent with growth. The sharp decline in Chl *a* after day 2 and the associated decline in phytoplankton abundance in the P alone treatment indicates that N was also in relatively short supply; as soon as the P was utilized, colimitation with respect to N and P developed. While our experiment does not provide direct evidence for the change toward N limitation following the drawdown of P in the P alone treatment, this explanation is consistent with the negligible N drawdown in the P addition experiment between days 2 and 3, and with the findings of other studies in this region [*C. M. Moore et al.*, 2013]. Indeed, P limitation has been suggested for the western North Atlantic based on enzyme activities [*Ammerman et al.*, 2003; *Lomas et al.*, 2004], low SRP concentrations [*Wu et al.*, 2000], high thermocline N:P ratios [*Fanning*, 1992], short P turnover times [*Sohm and Capone*, 2010], fast uptake rates [*Sohm and Capone*, 2006], extensive utilization of dissolved organic P [*Lomas et al.*, 2010; *McLaughlin et al.*, 2013], low abundance of phospholipids in resident phytoplankton [*Van Mooy et al.*, 2009], efficient physiological P acquisition mechanisms [*Martiny et al.*, 2006; *Scanlan and Wilson*, 1999] and the presence of intracellular polyphosphate [*Martin et al.*, 2014]. Phosphorus limitation in this region is also consistent with previous model results [*Krishnamurthy et al.*, 2007]. For example, both the Marine Ecosystem Dynamics and Biogeochemical Cycling Community Earth System Model (CESM1(BGC) [*J. K. Moore et al.*, 2013] and the MITgcm Darwin Project model (this study, as well as *Dutkiewicz et al.* [2014]) identify this region as one of the few areas of P limitation in the open ocean, particularly for diazotrophs but also for other phytoplankton. The decline in Chl *a* observed in the P addition experiments once N was depleted suggests that N is also in low abundance and may explain why other studies have identified this area as N and P limited [*C. M. Moore et al.*, 2013]. The timing of the Chl *a* decline in the P alone addition (low N:P ratio) is also consistent with previous work which demonstrates that the length of time some *Prochlorococcus* strains (the most abundant photosynthetic organism in the incubation water) stay in stationary phase (i.e., how quickly they crash) is a function of the N:P ratio. Specifically, *Moore et al.* [2002] show that some strains (NATL1. NATL2, MIT9211, and MIT9215) crashed within 2 days when N was limited.

Bacterial growth and respiration have also been shown to be stimulated by Saharan dust [*Pulido-Villena et al.*, 2014] and SRP additions [*Cotner et al.*, 1997; *Obernosterer et al.*, 2003] and could have contributed to P drawdown in the P addition experiments, although we did not measure changes in bacterial productivity or abundance. The diazotrophic cyanobacterium *Trichodesmium* spp. also appears to be P limited in this basin [*Sañudo-Wilhelmy et al.*, 2001; *Sohm et al.*, 2008] but was not detected in our samples. Note that the experimental design is different from the experiment carried out by *Thingstad et al.* [2005] in which grazing was implicated as the cause for Chl *a* decline, as we filtered out grazers larger than 20 μm before incubation. While smaller grazers could pass through the mesh in this experiment, it seems unlikely that they would cause a decline in Chl *a* only in the P alone treatment, but not in the N + P treatment (Figure 1). Thus our incubation experiments are consistent with the currently available body of research that indicates that biomass growth in this region is limited by P and that different organisms within the community could be colimited by N and P.

### 5.2. Taxa-Specific Responses to Nutrient Additions

In our study, Chl *a* concentrations by day 2 show a substantial increase in treatments to which P was added (and not with other additions); however, flow cytometry data suggest that not all phytoplankton taxa responded similarly. *Synechococcus* and picoeukaryote populations both increased in cell number and fluorescence (Figures 2a and 2b). *Synechococcus* showed the fastest response, increasing in the P alone treatment after only 2 days of incubation (Figure 2a). Similar increases in *Synechococcus* have been recorded in incubations from this region before [*Moore et al.*, 2008]. *Prochlorococcus*, however, shows a much smaller increase in both cell numbers and fluorescence relative to the control. *Prochlorococcus* was the most abundant photosynthetic organism in the water at the time of our sampling, and they did not respond strongly to any of the amendments in the bioassay incubation. This suggests that *Prochlorococcus* is more adapted to survive in the low nutrient, P-deficient waters of the western Tropical Atlantic Ocean and that they have acclimatized for coping with low P concentrations and high N:P ratio conditions. Higher surface area to volume ratio, increased nutrient uptake efficiency [*C. M. Moore et al.*, 2013], lower P requirements [*Morris et al.*, 2012; *Van Mooy et al.*, 2006], and efficient P acquisition, regulation, and utilization pathways [*Martiny et al.*, 2009] all give *Prochlorococcus* an advantage in low P waters. These mechanisms include using less P in cellular building blocks, storing P intracellularly as storage compounds to be reused later (e.g., polyphosphate)

[*Martin et al*., 2014], using organic P compounds, and having efficient P acquisition abilities (transporters). When P or N + P were added in our experiments, *Synechococcus* and picoeukaryotes, which did not bloom under the natural P-limited conditions, were able to grow faster because the added P shifted the nutrient regime away from P limitation, thereby opening a new niche. This suggests that addition of P in the incubation increased biomass by enhancing the growth rates of *Synechococcus* and picoeukaryotes while providing little immediate benefit for *Prochlorococcus* (Figure 2). Rather, *Prochlorococcus* initially dominated the community because it is adapted to the naturally P-limited conditions, and the cells were likely already operating at their maximum growth rate. Moreover, the higher proportion of $NH_4^+$ relative to $NO_3^-$ in aerosols in this region may benefit *Prochlorococcus*, due to its high affinity $NH_4^+$ transporters and preference for $NH_4^+$ [*García-Fernández et al*., 2004].

In this area, despite high atmospheric input of nutrients, P requirements for the other taxa are not met. To test if our conclusion (e.g., that relative nutrient availabilities dictate taxa distribution favoring *Prochlorococcus* in regions of low P and high N:P ratio) is consistent with global coupled atmosphere–ocean-ecosystem models, we used the MITgcm Darwin Project model as described above, specifically testing the effect of taxon-specific nutrient ratios and quotas. The model results were consistent with the bioassay results where *Synechococcus* and picoeukaryotes were P limited (Figure 2), and where *Prochlorococcus* dominates due to low P requirements and low P availability that is driven by atmospheric deposition in our study region (red box in Figure 5). The Mediterranean Sea, another LNLC area with high dust deposition and low P availability, showed a similar response to our study area, but other ocean regions did not. This was also true in a further experiment (see Figure S3) where we removed the dust supply of N and P; *Prochlorococcus* was the only species affected.

### 5.3. Atmospheric Deposition Control of Nutrient Ratios and Species Abundance

The ratio of N + N to SRP in aerosol samples used in our experiment ranged from 43:1 in the spring to 132:1 in summer, much higher than Redfield ratio (16:1). The ratios in aerosols are even higher when considering $NO_3^-$ and $NH_4^+$ together: both are typically present at similar concentrations in aerosols [*Zamora et al*., 2011]. Both N species are bio-available and utilized by phytoplankton. These ratios are consistent with the high ratios previously reported for aerosols collected in this region over the past two decades [*Baker et al*., 2010; *Zamora et al*., 2013] and with the relatively low phosphate solubility of African dust over this region (~8%) [*Zamora et al*., 2013]. This high N:P ratio in the soluble fraction of atmospheric deposition throughout the world's ocean is simulated in the atmospheric deposition models we used (Figure 3b) and fits other model predictions [*Okin et al*., 2011] and many observations of aerosol chemistry throughout the world [*Baker et al*., 2003; *Baker et al*., 2007; *Chen et al*., 2007; *Mackey et al*., 2013; *Markaki et al*., 2003; *Paytan et al*., 2009; *Srinivas and Sarin*, 2013]. Although we used only dry deposition in our incubation experiment, similarly high N:P values have been reported for wet deposition in this region [*Zamora et al*., 2013] and elsewhere [*Altieri et al*., 2009; *Markaki et al*., 2003; *Özsoy*, 2003; *Williams et al*., 1997; *Zhang et al*., 2008].

We argue that in this specific region the high N:P ratio in atmospheric deposition sustains the observed P limitation. This is because the N supplied by atmospheric deposition, in this region of relatively high atmospheric deposition and limited nutrient supply from other sources, constitutes a relatively large fraction of the total new N input to the euphotic zone (Table 5 and Figure 4), thereby maintaining a high N:P ratio in the surface ocean. Other external input sources (e.g., upwelling, river plumes) have much lower N:P ratios. *Prochlorococcus*, with its low P requirement and efficient P utilization has an advantage in areas of low P and high N:P ratios. Diazotrophs may be P limited and are less competitive in high N:P regions [*C. M. Moore et al*., 2013], as seen in the modeling study of *Dutkiewicz et al*. [2014]. Indeed, the occasional influx of nutrient rich water from the Orinoco and Amazon Rivers [*Mullerkarger et al*., 1989], which have higher P levels and lower N:P ratios, have been linked to increases in both *Trichodesmium* and diatom abundance in this region [*Borstad*, 1982a, 1982b; *Mullerkarger et al*., 1989; *Steven and Glombitz*, 1972; *Subramaniam et al*., 2008]. The stable stratification and shallow mixing depth limit the input of deeper water with N:P ratios closer to Redfield when compared to other oceanic settings [*Blain et al*., 2015; *Flohr et al*., 2014], and this enhances the effect that atmospheric deposition has in controlling surface N:P ratios. High N:P ratios in the euphotic zone and in sinking particulate matter, along with a positive N* ($N^* = (N - 16P + 2.90\ \mu mol\ kg^{-1})0.87$), see *Gruber and Sarmiento* [1997]) for subsurface water in this region (and throughout the North Atlantic subtropical thermocline) have also been observed [*Hansell and Follows*, 2008; *Hansell et al*., 2004, 2007] and are consistent with addition of more N relative to P. The idea that atmospheric deposition contributes to high

N:P ratios in this region is also consistent with the observed relationship between excess N in the water column of the Sargasso Sea and the North Atlantic Oscillation (NAO) [*Bates and Hansell*, 2004], because the magnitude and timing of atmospheric transport to the region is affected by NAO-related changes in atmospheric circulation. The high excess N in the eastern tropical South Atlantic [*Hansell et al*., 2004] could also be explained by high atmospheric deposition rates off the west coast of Africa.

The potential role of atmospheric deposition as a new N source has been previously recognized [*Duce et al*., 2008]; however, it was suggested that due to low atmospheric deposition fluxes relative to other nutrient sources, atmospheric deposition would have relatively little direct impact on open ocean biota [*Knap et al*., 1986; *Krishnamurthy et al*., 2009; *Michaels et al*., 1993]. Moreover, most previous studies have attributed the excess N, high N:P, and low $\delta^{15}N$ signatures in $NO_3^-$ seen in this region to nitrogen fixation [*Hansell et al*., 2004; *Knapp et al*., 2008; *Wu et al*., 2000]. The contributions from atmospheric N deposition and $N_2$ fixation have similar biogeochemical signatures (low N isotope and high N:P ratios) and thus are difficult to differentiate [*Hansell et al*., 2007; *Knapp et al*., 2010]. Our incubation results, however, suggest that N from atmospheric deposition, or more specifically the high N:P ratio in atmospheric deposition, could enable *Prochlorococcus* to outcompete diazotrophs. In fact, the high N:P ratios (and low P concentrations) could in themselves limit the activity of diazotrophs [*Mills et al*., 2004; *Sañudo-Wilhelmy et al*., 2001; *Voss et al*., 2004]; hence, it is likely that at least part of the observed excess N in the subsurface and low $\delta^{15}N$ of $NO_3^-$ in this region is a result of direct input of N from atmospheric deposition sources.

Atmospheric deposition of N, P, and Fe (Figure 3a), as well as the associated N:P and N:Fe ratios (Figure 3b), vary considerably in space. This is due to the different sources of these elements in aerosols. The relatively high contribution of aeolian (mineral dust) deposition in the North Atlantic, and specifically in our study site (where other new N sources are small), results in both a high N:P ratio and a high excess N input (relative to P) to the euphotic zone (Table 5). Our model results, which take into account variability in the stoichiometry of nutrient supply as well as phytoplankton group specific demand, indicate that aerosol deposition not only impacts but plays a major role in phytoplankton community structure in the LNLC regions of the west tropical North Atlantic Ocean by controlling nutrient distribution in surface seawater, particularly by maintaining high N:P ratios and high Fe. Specifically, including phytoplankton taxon-specific C:N:P in conjunction with N, P, and Fe in atmospheric deposition had a large impact on the distributions of phytoplankton taxa, as shown by comparing these results to model outputs that do not include variable nutrient stoichiometry demand (Figure 5). The largest impact in our region is an increase in *Prochlorococcus* relative to higher-latitude waters. Previous model studies [e.g., *Krishnamurthy et al*., 2010] have shown that the addition of aeolian N and P sources does not produce a large change in global productivity or phytoplankton distributions (see supporting information Figure S3). However, here we show that there is a change in phytoplankton community structure in the North Atlantic subtropical gyre, specifically in the region where the contribution of atmospheric nutrients is greatest relative to other sources. Here *Prochlorococcus* benefits because of its low P requirement relative to N, and as a result their abundance is higher, particularly in the central portion of the region (Figure 5d).

## 6. Summary and Implications

Direct observations and modeling results suggest that high atmospheric deposition rates and N:P ratios in the Caribbean Sea create conditions that favor phytoplankton with low P requirements and efficient P acquisition strategies, such as *Prochlorococcus*. This work provides insight into the observation that the southwestern North Atlantic is characterized by relatively low productivity and high abundance of *Prochlorococcus* and demonstrates the impact of atmospheric nutrients in this LNLC area. Similar conditions prevail in the Mediterranean Sea and the Gulf of Aqaba, Red Sea, where *Prochlorococcus* is also prevalent. Models predict that future climate will enhance ocean stratification [*Sarmiento et al*., 2004; *Steinacher et al*., 2010], and N loading in aerosols is also expected to increase [*Duce et al*., 2008; *Gruber and Galloway*, 2008; *Krishnamurthy et al*., 2009]. Based on our observations, this may impact phytoplankton community structure and productivity in some regions of the ocean, most notably regions that are close to being P limited. Indeed a recent study has already detected changes that are consistent with higher anthropogenic N deposition and expansion of P limitation [*Kim et al*., 2014]. This may also have cascading impacts on other processes such as carbon export to depth because particle sinking rates in systems characterized by small cells are slow [*Bach et al*., 2012].

**Acknowledgments**
We thank the Bellairs Research Institute for providing accommodation, laboratory space, and supplies in Barbados. This work was supported by NSF-OCE grant 0850467 to Adina Paytan. The data supporting this work are listed in the tables, figures, and supporting information.

## References

Altieri, K. E., B. J. Turpin, and S. P. Seitzinger (2009), Composition of dissolved organic nitrogen in continental precipitation investigated by ultra-high resolution FT-ICR mass spectrometry, *Environ. Sci. Technol.*, *43*(18), 6950–6955, doi:10.1021/es9007849.

Ammerman, J. W., R. R. Hood, D. A. Case, and J. B. Cotner (2003), Phosphorus deficiency in the Atlantic: An emerging paradigm in oceanography, *Eos Trans. AGU*, *84*(18), 165–170, doi:10.1029/2003EO180001.

Anderson, L. D., K. L. Faul, and A. Paytan (2010), Phosphorus associations in aerosols: What can they tell us about P bioavailability?, *Mar. Chem.*, *120*(1–4), 44–56, doi:10.1016/j.marchem.2009.04.008.

Armstrong, F. A. J., C. R. Stearns, and J. D. H. Strickland (1967), The measurement of upwelling and subsequent biological process by means of the Technicon Autoanalyzer® and associated equipment, *Deep Sea Res. Oceanogr. Abstr.*, *14*(3), 381–389, doi:10.1016/0011-7471(67)90082-4.

Bach, L. T., U. Riebesell, S. Sett, S. Febiri, P. Rzepka, and K. G. Schulz (2012), An approach for particle sinking velocity measurements in the 3–400 μm size range and considerations on the effect of temperature on sinking rates, *Marine Biol.*, *159*(8), 1853–1864, doi:10.1007/s00227-012-1945-2.

Baker, A. R., and P. L. Croot (2010), Atmospheric and marine controls on aerosol iron solubility in seawater, *Mar. Chem.*, *120*(1–4), 4–13, doi:10.1016/j.marchem.2008.09.003.

Baker, A. R., S. D. Kelly, K. F. Biswas, M. Witt, and T. D. Jickells (2003), Atmospheric deposition of nutrients to the Atlantic Ocean, *Geophys. Res. Lett.*, *30*(24), 2296, doi:10.1029/2003GL018518.

Baker, A. R., M. French, and K. L. Linge (2006a), Trends in aerosol nutrient solubility along a west–east transect of the Saharan dust plume, *Geophys. Res. Lett.*, *33*, L07805, doi:10.1029/2005GL024764.

Baker, A. R., T. D. Jickells, M. Witt, and K. L. Linge (2006b), Trends in the solubility of iron, aluminium, manganese and phosphorus in aerosol collected over the Atlantic Ocean, *Mar. Chem.*, *98*(1), 43–58, doi:10.1016/j.marchem.2005.06.004.

Baker, A. R., K. Weston, S. D. Kelly, M. Voss, P. Streu, and J. N. Cape (2007), Dry and wet deposition of nutrients from the tropical Atlantic atmosphere: Links to primary productivity and nitrogen fixation, *Deep Sea Res., Part I*, *54*(10), 1704–1720, doi:10.1016/j.dsr.2007.07.001.

Baker, A. R., T. Lesworth, C. Adams, T. D. Jickells, and L. Ganzeveld (2010), Estimation of atmospheric nutrient inputs to the Atlantic Ocean from 50°N to 50°S based on large-scale field sampling: Fixed nitrogen and dry deposition of phosphorus, *Global Biogeochem. Cycles*, *24*, GB3006, doi:10.1029/2009GB003634.

Bates, N. R., and D. A. Hansell (2004), Temporal variability of excess nitrate in the subtropical mode water of the North Atlantic Ocean, *Mar. Chem.*, *84*(3), 225–241.

Bernhardt, H., and A. Wilhelms (1967), The continuous determination of low level iron, soluble phosphate and total phosphate with the AutoAnalyzer, paper presented at Technicon Symposia., *1*, 385–389.

Biller, D. V., and K. W. Bruland (2012), Analysis of Mn, Fe, Co, Ni, Cu, Zn, Cd, and Pb in seawater using the Nobias-chelate PA1 resin and magnetic sector inductively coupled plasma mass spectrometry (ICP-MS), *Mar. Chem.*, *130*, 12–20, doi:10.1016/j.marchem.2011.12.001.

Bishop, J. K. B., R. E. Davis, and J. T. Sherman (2002), Robotic observations of dust storm enhancement of carbon biomass in the North Pacific, *Science*, *298*(5594), 817–821, doi:10.1126/science.1074961.

Blain, S., J. Capparos, A. Guéneuguès, I. Obernosterer, and L. Oriol (2015), Distributions and stoichiometry of dissolved nitrogen and phosphorus in the iron-fertilized region near Kerguelen (Southern Ocean), *Biogeosciences*, *12*(2), 623–635.

Borstad, G. A. (1982a), The influence of the meandering Guiana Current on surface conditions near Barbados—Temporal variations of *Trichodesmium* (Cyanophyta) and other plankton, *J. Mar. Res.*, *40*(2), 435–452.

Borstad, G. A. (1982b), The influence of the meandering Guiana Current and Amazon River discharge on surface salinity near Barbados, *J. Mar. Res.*, *40*(2), 421–434.

Boyd, P. W., C. S. Wong, J. Merrill, F. Whitney, J. Snow, P. J. Harrison, and J. Gower (1998), Atmospheric iron supply and enhanced vertical carbon flux in the NE subarctic Pacific: Is there a connection?, *Global Biogeochem. Cycles*, *12*(3), 429–441, doi:10.1029/98GB00745.

Boyd, P. W., D. S. Mackie, and K. A. Hunter (2010), Aerosol iron deposition to the surface ocean—Modes of iron supply and biological responses, *Mar. Chem.*, *120*(1–4), 128–143, doi:10.1016/j.marchem.2009.01.008.

Bressac, M., C. Guieu, D. Doxaran, F. Bourrin, K. Desboeufs, N. Leblond, and C. Ridame (2014), Quantification of the lithogenic carbon pump following a simulated dust-deposition event in large mesocosms, *Biogeosciences*, *11*(4), 1007–1020, doi:10.5194/bg-11-1007-2014.

Bristow, C. S., K. A. Hudson-Edwards, and A. Chappell (2010), Fertilizing the Amazon and equatorial Atlantic with West African dust, *Geophys. Res. Lett.*, *37*, L14807, doi:10.1029/2010GL043486.

Chen, Y., J. Street, and A. Paytan (2006), Comparison between pure-water-and seawater-soluble nutrient concentrations of aerosols from the Gulf of Aqaba, *Mar. Chem.*, *101*(1), 141–152.

Chen, Y., S. Mills, J. Street, D. Golan, A. Post, M. Jacobson, and A. Paytan (2007), Estimates of atmospheric dry deposition and associated input of nutrients to Gulf of Aqaba seawater, *J. Geophys. Res.*, *112*, D04309, doi:10.1029/2006JD007858.

Cotner, J. B., J. W. Ammerman, E. R. Peele, and E. Bentzen (1997), Phosphorus-limited bacterioplankton growth in the Sargasso Sea, *Aquat. Microb. Ecol.*, *13*(2), 141–149, doi:10.3354/ame013141.

Dandonneau, Y., P.-Y. Deschamps, J.-M. Nicolas, H. Loisel, J. Blanchot, Y. Montel, F. Thieuleux, and G. Bécu (2004), Seasonal and interannual variability of ocean color and composition of phytoplankton communities in the North Atlantic, equatorial Pacific and South Pacific, *Deep Sea Res. Part II*, *51*(1–3), 303–318, doi:10.1016/j.dsr2.2003.07.018.

Dentener, F., et al. (2006), Nitrogen and sulfur deposition on regional and global scales: A multimodel evaluation, *Global Biogeochem. Cycles*, *20*, GB4003, doi:10.1029/2005GB002672.

Duarte, C. M., J. Dachs, M. Llabrés, P. Alonso-Laita, J. M. Gasol, A. Tovar-Sánchez, S. Sañudo-Wilhemy, and S. Agustí (2006), Aerosol inputs enhance new production in the subtropical northeast Atlantic, *J. Geophys. Res.*, *111*, G04006, doi:10.1029/2005JG000140.

Duce, R. A., et al. (1991), The atmospheric input of trace species to the world ocean, *Global Biogeochem. Cycles*, *5*(3), 193–260, doi:10.1029/91GB01778.

Duce, R. A., et al. (2008), Impacts of atmospheric anthropogenic nitrogen on the open ocean, *Science*, *320*(5878), 893–897, doi:10.1126/science.1150369.

Dutkiewicz, S., B. A. Ward, J. R. Scott, and M. J. Follows (2014), Understanding predicted shifts in diazotroph biogeography using resource competition theory, *Biogeosciences*, *11*(19), 5445–5461, doi:10.5194/bg-11-5445-2014.

Dutkiewicz, S., A. E. Hickman, O. Jahn, W. W. Gregg, C. B. Mouw, and M. J. Follows (2015), Capturing optically important constituents and properties in a marine biogeochemical and ecosystem model, *Biogeosci. Discuss.*, *12*(3), 2607–2695, doi:10.5194/bgd-12-2607-2015.

Elrod, V. A., W. M. Berelson, K. H. Coale, and K. S. Johnson (2004), The flux of iron from continental shelf sediments: A missing source for global budgets, *Geophys. Res. Lett.*, *31*, L12307, doi:10.1029/2004GL020216.

Erickson, D. J., J. L. Hernandez, P. Ginoux, W. W. Gregg, C. McClain, and J. Christian (2003), Atmospheric iron delivery and surface ocean biological activity in the Southern Ocean and Patagonian region, *Geophys. Res. Lett.*, *30*(12), 1609, doi:10.1029/2003GL017241.

Fanning, K. A. (1992), Nutrient provinces in the sea: Concentration ratios, reaction rate ratios, and ideal covariation, *J. Geophys. Res.*, *97*(C4), 5693–5712, doi:10.1029/92JC00007.

Fitzsimmons, J. N., R. Zhang, and E. A. Boyle (2013), Dissolved iron in the tropical North Atlantic Ocean, *Mar. Chem.*, *154*, 87–99, doi:10.1016/j.marchem.2013.05.009.

Flohr, A., A. K. van der Plas, K. C. Emeis, V. Mohrholz, and T. Rixen (2014), Spatio-temporal patterns of C:N:P ratios in the northern Benguela upwelling system, *Biogeosciences*, *11*(3), 885–897, doi:10.5194/bg-11-885-2014.

Garcia, H. E., Locarnini, R. A., Boyer, T. P., and Antonov, J. I. (2006), World Ocean Atlas 2005, vol. 4, Nutrients (phosphate, nitrate, silicate), NOAA Atlas NESDIS, *64*, 396, edited by S. Levitus, NOAA, Silver Spring, Md.

Garcia, H. E., R. A. Locarnini, T. P. Boyer, J. I. Antonov, M. M. Zweng, O. K. Baranova, and D. R. Johnson (2010), World Ocean Atlas 2009, Volume 4: Nutrients (phosphate, nitrate, and silicate), *NOAA Atlas NESDIS 71*, vol. 4, edited by S. Levitus, 398 pp., U.S. Govt. Print. Off., Washington, D. C.

García-Fernández, J. M., N. T. de Marsac, and J. Diez (2004), Streamlined regulation and gene loss as adaptive mechanisms in *Prochlorococcus* for optimized nitrogen utilization in oligotrophic environments, *Microbiol. Mol. Biol. Rev.*, *68*(4), 630–638.

Ginoux, P., J. M. Prospero, T. E. Gill, N. C. Hsu, and M. Zhao (2012), Global-scale attribution of anthropogenic and natural dust sources and their emission rates based on MODIS Deep Blue aerosol products, *Rev. Geophys.*, *50*, RG3005, doi:10.1029/2012RG000388.

Giovagnetti, V., C. Brunet, F. Conversano, F. Tramontano, I. Obernosterer, C. Ridame, and C. Guieu (2013), Assessing the role of dust deposition on phytoplankton ecophysiology and succession in a low-nutrient low-chlorophyll ecosystem: A mesocosm experiment in the Mediterranean Sea, *Biogeosciences*, *10*(5), 2973–2991, doi:10.5194/bg-10-2973-2013.

Gruber, N., and J. L. Sarmiento (1997), Global patterns of marine nitrogen fixation and denitrification, *Global Biogeochem. Cycles*, *11*(2), 235–266, doi:10.1029/97GB00077.

Gruber, N., and J. N. Galloway (2008), An Earth-system perspective of the global nitrogen cycle, *Nature*, *451*(7176), 293–296.

Guieu, C., F. Dulac, C. Ridame, and P. Pondaven (2014a), Introduction to project DUNE, a DUst experiment in a low Nutrient, low chlorophyll Ecosystem, *Biogeosciences*, *11*(2), 425–442, doi:10.5194/bg-11-425-2014.

Guieu, C., C. Ridame, E. Pulido-Villena, M. Bressac, K. Desboeufs, and F. Dulac (2014b), Dust deposition in an oligotrophic marine environment: Impact on the carbon budget, *Biogeosci. Discuss.*, *11*(1), 1707–1738, doi:10.5194/bgd-11-1707-2014.

Guo, C., J. Yu, T. Y. Ho, L. Wang, S. Song, L. Kong, and H. Liu (2012), Dynamics of phytoplankton community structure in the South China Sea in response to the East Asian aerosol input, *Biogeosciences*, *9*(4), 1519–1536, doi:10.5194/bg-9-1519-2012.

Hans Wedepohl, K. (1995), The composition of the continental crust, *Geochim. Cosmochim. Acta*, *59*(7), 1217–1232, doi:10.1016/0016-7037(95)00038-2.

Hansell, D. A., and M. J. Follows (2008), Nitrogen in the Atlantic Ocean, Chapter 13, in *Nitrogen in the Marine Environment*, 2nd ed., Elsevier Inc., doi:10.1016/B978-0-12-372522-6.00013-X.

Hansell, D. A., N. R. Bates, and D. B. Olson (2004), Excess nitrate and nitrogen fixation in the North Atlantic Ocean, *Mar. Chem.*, *84*(3–4), 243–265, doi:10.1016/j.marchem.2003.08.004.

Hansell, D. A., D. B. Olson, F. Dentener, and L. M. Zamora (2007), Assessment of excess nitrate development in the subtropical North Atlantic, *Mar. Chem.*, *106*(3–4), 562–579, doi:10.1016/j.marchem.2007.06.005.

Henson, S. A., J. L. Sarmiento, J. P. Dunne, L. Bopp, I. Lima, S. C. Doney, J. John, and C. Beaulieu (2010), Detection of anthropogenic climate change in satellite records of ocean chlorophyll and productivity, *Biogeosciences*, *7*(2), 621–640, doi:10.5194/bg-7-621-2010.

Hodge, V., S. R. Johnson, and E. D. Goldberg (1978), Influence of atmospherically transported aerosols on surface ocean water composition, *Geochem. J.*, *12*(1), 7–20.

Husar, R. B., J. M. Prospero, and L. L. Stowe (1997), Characterization of tropospheric aerosols over the oceans with the NOAA advanced very high resolution radiometer optical thickness operational product, *J. Geophys. Res.*, *102*(D14), 16,889–16,909, doi:10.1029/96JD04009.

Jickells, T. D., et al. (2005), Global iron connections between desert dust, ocean biogeochemistry, and climate, *Science*, *308*(5718), 67–71, doi:10.1126/science.1105959.

Jordi, A., G. Basterretxea, A. Tovar-Sánchez, A. Alastuey, and X. Querol (2012), Copper aerosols inhibit phytoplankton growth in the Mediterranean Sea, *Proc. Natl. Acad. Sci. U.S.A.*, doi:10.1073/pnas.1207567110.

Jung, E., B. Albrecht, J. M. Prospero, H. H. Jonsson, and S. M. Kreidenweis (2013), Vertical structure of aerosols, temperature, and moisture associated with an intense African dust event observed over the eastern Caribbean, *J. Geophys. Res. Atmos.*, *118*, 4623–4643, doi:10.1002/jgrd.50352.

Kanakidou, M., et al. (2012), Atmospheric fluxes of organic N and P to the global ocean, *Global Biogeochem. Cycles*, *26*, doi:10.1029/2011GB004277.

Kim, I.-N., K. Lee, N. Gruber, D. M. Karl, J. L. Bullister, S. Yang, and T.-W. Kim (2014), Increasing anthropogenic nitrogen in the North Pacific Ocean, *Science*, *346*(6213), 1102–1106, doi:10.1126/science.1258396.

Knap, A., T. Jickells, A. Pszenny, and J. Galloway (1986), Significance of atmospheric-derived fixed nitrogen on productivity of the Sargasso Sea, *Nature*, *320*(6058), 158–160.

Knapp, A. N., P. J. DiFiore, C. Deutsch, D. M. Sigman, and F. Lipschultz (2008), Nitrate isotopic composition between Bermuda and Puerto Rico: Implications for N2 fixation in the Atlantic Ocean, *Global Biogeochem. Cycles*, *22*, GB3014, doi:10.1029/2007GB003107.

Knapp, A. N., M. G. Hastings, D. M. Sigman, F. Lipschultz, and J. N. Galloway (2010), The flux and isotopic composition of reduced and total nitrogen in Bermuda rain, *Mar. Chem.*, *120*(1–4), 83–89, doi:10.1016/j.marchem.2008.08.007.

Krishnamurthy, A., J. K. Moore, C. S. Zender, and C. Luo (2007), Effects of atmospheric inorganic nitrogen deposition on ocean biogeochemistry, *J. Geophys. Res.*, *112*, G02019, doi:10.1029/2006JG000334.

Krishnamurthy, A., J. K. Moore, N. Mahowald, C. Luo, S. C. Doney, K. Lindsay, and C. S. Zender (2009), Impacts of increasing anthropogenic soluble iron and nitrogen deposition on ocean biogeochemistry, *Global Biogeochem. Cycles*, *23*, GB3016, doi:10.1029/2008GB003440.

Krishnamurthy, A., J. K. Moore, N. Mahowald, C. Luo, and C. S. Zender (2010), Impacts of atmospheric nutrient inputs on marine biogeochemistry, *J. Geophys. Res.*, *115*, G01006, doi:10.1029/2009JG001115.

Lamarque, J. F., et al. (2011), CAM-chem: Description and evaluation of interactive amtopsheric chemistry in CESM, *Geosci. Model Dev.*, *4*, 2199–2278.

Lamarque, J.-F., et al. (2010), Historical (1850–2000) gridded anthropogenic and biomass burning emissions of reactive gases and aerosols: methodology and application, *Atmos. Chem. Phys.*, *10*(7017), 7017–7039.

Lomas, M. W., A. Swain, R. Shelton, and J. W. Ammerman (2004), Taxonomic variability of phosphorus stress in Sargasso Sea phytoplankton, *Limnol. Oceanogr.*, *49*(6), 2303–2310.

Lomas, M. W., A. L. Burke, D. A. Lomas, D. W. Bell, C. Shen, S. T. Dyhrman, and J. W. Ammerman (2010), Sargasso Sea phosphorus biogeochemistry: An important role for dissolved organic phosphorus (DOP), *Biogeosciences*, *7*(2), 695–710, doi:10.5194/bg-7-695-2010.

Luo, C., N. Mahowald, T. Bond, P. Y. Chuang, P. Artaxo, R. Siefert, Y. Chen, and J. Schauer (2008), Combustion iron distribution and deposition, *Global Biogeochem. Cycles*, *22*, GB1012, doi:10.1029/2007GB002964.

Mackey, K. R. M., K. Roberts, M. W. Lomas, M. A. Saito, A. F. Post, and A. Paytan (2012a), Enhanced solubility and ecological impact of atmospheric phosphorus deposition upon extended seawater exposure, *Environ. Sci. Technol.*, *46*(19), 10,438–10,446, doi:10.1021/es3007996.

Mackey, K. R. M., K. N. Buck, J. R. Casey, A. Cid, M. W. Lomas, Y. Sohrin, and A. Paytan (2012b), Phytoplankton responses to atmospheric metal deposition in the coastal and open-ocean Sargasso Sea, *Front. Microbiol.*, *3*, 359, doi:10.3389/fmicb.2012.00359.
Mackey, K. R. M., D. Hunter, E. V. Fischer, Y. Jiang, B. Allen, Y. Chen, A. Liston, J. Reuter, G. Schladow, and A. Paytan (2013), Aerosol-nutrient-induced picoplankton growth in Lake Tahoe, *J. Geophys. Res. Biogeosci.*, *118*, 1054–1067, doi:10.1002/jgrg.20084.
Mackey, K. R. M., C. T. Chien, A. F. Post, M. A. Saito, and A. Paytan (2015a), Rapid and gradual modes of aerosol trace metal dissolution in seawater, *Front. Microbiol.*, *5*, 794, doi:10.3389/fmicb.2014.00794.
Mackey, K. R. M., A. F. Post, M. R. McIlvin, G. A. Cutter, S. G. John, and M. A. Saito (2015b), Divergent responses of Atlantic coastal and oceanic *Synechococcus* to iron limitation, *Proc. Natl. Acad. Sci. U.S.A.*, *112*(32), 9944–9949.
Mahowald, N., et al. (2008), The global distribution of atmospheric phosphorus deposition and anthropogenic impacts, *Global Biogeochem. Cycles*, *22*, GB4026, doi:10.1029/2008GB003240.
Mahowald, N. M., A. R. Baker, G. Bergametti, N. Brooks, R. A. Duce, T. D. Jickells, N. Kubilay, J. M. Prospero, and I. Tegen (2005), Atmospheric global dust cycle and iron inputs to the ocean, *Global Biogeochem. Cycles*, *19*, GB2005, doi:10.1029/2004GB002402.
Mahowald, N. M., D. Muhs, S. Levis, P. Rasch, M. Yoshioka, and C. Zender (2006), Change in atmospheric mineral aerosols in response to climate: Last glacial period, pre-industrial, modern and doubled-carbon dioxide climates, *J. Geophys. Res.*, *111*, D10202, doi:10.1029/12005JD006653.
Mahowald, N. M., J. A. Ballantine, J. Feddema, and N. Ramankutty (2007), Global trends in visibility: Implications for dust sources, *Atmos. Chem. Phys.*, *7*(12), 3309–3339, doi:10.5194/acp-7-3309-2007.
Mahowald, N. M., et al. (2009), Atmospheric iron deposition: global distribution, variability, and human perturbations, *Annu. Rev. Mar. Sci.*, *1*, 245–278.
Mahowald, N. M., et al. (2010), Observed 20th century desert dust variability: Impact on climate and biogeochemistry, *Atmos. Chem. Phys.*, *10*(22), 10,875–10,893, doi:10.5194/acp-10-10875-2010.
Mann, E. L., N. Ahlgren, J. W. Moffett, and S. W. Chisholm (2002), Copper toxicity and cyanobacteria ecology in the Sargasso Sea, *Limnol. Oceanogr.*, *47*(4), 976–988.
Maranon, E., et al. (2010), Degree of oligotrophy controls the response of microbial plankton to Saharan dust, *Limnol. Oceanogr.*, *55*(6), 2339–2352, doi:10.4319/lo.2010.55.6.2339.
Markaki, Z., K. Oikonomou, M. Kocak, G. Kouvarakis, A. Chaniotaki, N. Kubilay, and N. Mihalopoulos (2003), Atmospheric deposition of inorganic phosphorus in the Levantine Basin, eastern Mediterranean: Spatial and temporal variability and its role in seawater productivity, *Limnol. Oceanogr.*, *48*(4), 1557–1568.
Marshall, J., A. Adcroft, C. Hill, L. Perelman, and C. Heisey (1997), A finite-volume, incompressible Navier Stokes model for studies of the ocean on parallel computers, *J. Geophys. Res.*, *102*(C3), 5753–5766, doi:10.1029/96JC02775.
Martin, P., S. T. Dyhrman, M. W. Lomas, N. J. Poulton, and B. A. S. Van Mooy (2014), Accumulation and enhanced cycling of polyphosphate by Sargasso Sea plankton in response to low phosphorus, *Proc. Natl. Acad. Sci. U.S.A.*, *111*(22), 8089–8094, doi:10.1073/pnas.1321719111.
Martiny, A. C., M. L. Coleman, and S. W. Chisholm (2006), Phosphate acquisition genes in *Prochlorococcus* ecotypes: Evidence for genome-wide adaptation, *Proc. Natl. Acad. Sci. U.S.A.*, *103*(33), 12,552–12,557, doi:10.1073/pnas.0601301103.
Martiny, A. C., Y. Huang, and W. Li (2009), Occurrence of phosphate acquisition genes in *Prochlorococcus* cells from different ocean regions, *Environ. Microbiol.*, *11*(6), 1340–1347, doi:10.1111/j.1462-2920.2009.01860.x.
Mawji, E., et al. (2015), The GEOTRACES intermediate data product 2014, *Mar. Chem.*, *177*, 1–8, doi:10.1016/j.marchem.2015.04.005.
McLaughlin, K., J. A. Sohm, G. A. Cutter, M. W. Lomas, and A. Paytan (2013), Phosphorus cycling in the Sargasso Sea: Investigation using the oxygen isotopic composition of phosphate, enzyme-labeled fluorescence, and turnover times, *Global Biogeochem. Cycles*, *27*, 375–387, doi:10.1002/gbc.20037.
Michaels, A. F., D. A. Siegel, R. J. Johnson, A. H. Knap, and J. N. Galloway (1993), Episodic inputs of atmospheric nitrogen to the Sargasso Sea: Contributions to new production and phytoplankton blooms, *Global Biogeochem. Cycles*, *7*(2), 339–351, doi:10.1029/93GB00178.
Mills, M. M., C. Ridame, M. Davey, J. La Roche, and R. J. Geider (2004), Iron and phosphorus co-limit nitrogen fixation in the eastern tropical North Atlantic, *Nature*, *429*(6989), 292–294, doi:10.1038/nature02550.
Moore, C. M., M. M. Mills, R. Langlois, A. Milne, E. P. Achterberg, J. La Roche, and R. J. Geider (2008), Relative influence of nitrogen and phosphorous availability on phytoplankton physiology and productivity in the oligotrophic sub-tropical North Atlantic Ocean, *Limnol. Oceanogr.*, *53*(1), 291–305, doi:10.4319/lo.2008.53.1.0291.
Moore, C. M., et al. (2013), Processes and patterns of oceanic nutrient limitation, *Nat. Geosci.*, *6*(9), 701–710, doi:10.1038/ngeo1765.
Moore, J. K., K. Lindsay, S. C. Doney, M. C. Long, and K. Misumi (2013), Marine ecosystem dynamics and biogeochemical cycling in the Community Earth System model [CESM1(BGC)]: Comparison of the 1990s with the 2090s under the RCP4.5 and RCP8.5 scenarios, *J. Clim.*, *26*(23), 9291–9312, doi:10.1175/JCLI-D-12-00566.1.
Moore, L. R., A. F. Post, G. Rocap, and S. W. Chisholm (2002), Utilization of different nitrogen sources by the marine cyanobacteria *Prochlorococcus* and *Synechococcus*, *Limnol. Oceanogr.*, *47*(4), 989–996.
Morel, F. M. M., J. R. Reinfelder, S. B. Roberts, C. P. Chamberlain, J. G. Lee, and D. Yee (1994), Zinc and carbon co-limitation of marine-phytoplankton, *Nature*, *369*(6483), 740–742, doi:10.1038/369740a0.
Morris, J. J., R. E. Lenski, and E. R. Zinser (2012), The black queen hypothesis: Evolution of dependencies through adaptive gene loss, *MBio*, *3*(2), e00036-12,
Morton, P. L., et al. (2013), Methods for the sampling and analysis of marine aerosols: Results from the 2008 GEOTRACES aerosol intercalibration experiment, *Limnol. Oceanogr. Methods*, *11*, 62–78, doi:10.4319/lom.2013.11.62.
Mullerkarger, F. E., C. R. McClain, and P. L. Richardson (1988), The dispersal of the amazons water, *Nature*, *333*(6168), 56–59, doi:10.1038/333056a0.
Mullerkarger, F. E., C. R. McClain, T. R. Fisher, W. E. Esaias, and R. Varela (1989), Pigment distribution in the Caribbean Sea - observation from space, *Prog. Oceanogr.*, *23*(1), 23–64, doi:10.1016/0079-6611(89)90024-4.
Neale, R., J. Richter, S. Park, P. Lauritzen, S. Vavrus, P. Rasch, and M. Zhang (2013), The mean climate of the Community Atmosphere Model (CAM4) in forced SST and fully copled experiments, *J. Clim.*, *26*, 5150–5168, doi:10.1175/JCLI-D-12-00236.1.
Obernosterer, I., N. Kawasaki, and R. Benner (2003), P-limitation of respiration in the Sargasso Sea and uncoupling of bacteria from P-regeneration in size-fractionation experiments, *Aquat. Microb. Ecol.*, *32*(3), 229–237, doi:10.3354/ame032229.
Okin, G. S., et al. (2011), Impacts of atmospheric nutrient deposition on marine productivity: Roles of nitrogen, phosphorus, and iron, *Global Biogeochem. Cycles*, *25*, GB2022, doi:10.1029/2010GB003858.
Oschlies, A., and V. Garcon (1998), Eddy-induced enhancement of primary production in a model of the North Atlantic Ocean, *Nature*, *394*(6690), 266–269.
Özsoy, T. (2003), Atmospheric wet deposition of soluble macro-nutrients in the Cilician Basin, north-eastern Mediterranean sea, *J. Environ. Monit.*, *5*(6), 971–976.

Parekh, P., M. J. Follows, and E. A. Boyle (2005), Decoupling of iron and phosphate in the global ocean, *Global Biogeochem. Cycles*, *19*, GB2020, doi:10.1029/2004GB002280.
Parekh, P., M. J. Follows, S. Dutkiewicz, and T. Ito (2006), Physical and biological regulation of the soft tissue carbon pump, *Paleoceanography*, *21*, PA3001, doi:10.1029/2005PA001258.
Paytan, A., K. R. M. Mackey, Y. Chen, I. D. Lima, S. C. Doney, N. Mahowald, R. Labiosa, and A. F. Postf (2009), Toxicity of atmospheric aerosols on marine phytoplankton, *Proc. Natl. Acad. Sci. U.S.A.*, *106*(12), 4601–4605, doi:10.1073/pnas.0811486106.
Prospero, J. M., K. Barrett, T. Church, F. Dentener, R. A. Duce, J. N. Galloway, H. Levy, J. Moody, and P. Quinn (1996), Atmospheric deposition of nutrients to the North Atlantic basin, *Biogeochemistry*, *35*(1), 27–73, doi:10.1007/bf02179824.
Prospero, J. M., F.-X. Collard, J. Molinié, and A. Jeannot (2014), Characterizing the annual cycle of African dust transport to the Caribbean Basin and South America and its impact on the environment and air quality, *Global Biogeochem. Cycles*, *28*, 757–773, doi:10.1002/2013GB004802.
Pulido-Villena, E., A. C. Baudoux, I. Obernosterer, M. Landa, J. Caparros, P. Catala, C. Georges, J. Harmand, and C. Guieu (2014), Microbial food web dynamics in response to a Saharan dust event: Results from a mesocosm study in the oligotrophic Mediterranean Sea, *Biogeosciences*, *11*(19), 5607–5619, doi:10.5194/bg-11-5607-2014.
Randerson, J. T., G. R. van der Werf, L. Giglio, G. J. Collatz, and P. S. Kasibhatla. (2013), Global fire emissions database, Version 3 (GFEDv3.1).
Rasch, P. J., W. D. Collins, and B. E. Eaton (2000), Understanding the Indian Ocean Experiment INDOEX aerosol distributions with an aerosol assimilation, *J. Geophys. Res.*, *106*(D7), 7337–7355, doi:10.1029/2000JD900508.
Rijkenberg, M. J. A., R. Middag, P. Laan, L. J. A. Gerringa, H. M. van Aken, V. Schoemann, J. T. M. de Jong, and H. J. W. de Baar (2014), The distribution of dissolved iron in the west Atlantic Ocean, *PLoS One*, *9*(6), e101323, doi:10.1371/journal.pone.0101323.
Saito, M. A., T. J. Goepfert, and J. T. Ritt (2008), Some thoughts on the concept of colimitation: Three definitions and the importance of bioavailability, *Limnol. Oceanogr.*, *53*(1), 276–290, doi:10.4319/lo.2008.53.1.0276.
Sañudo-Wilhelmy, S. A., A. B. Kustka, C. J. Gobler, D. A. Hutchins, M. Yang, K. Lwiza, J. Burns, D. G. Capone, J. A. Raven, and E. J. Carpenter (2001), Phosphorus limitation of nitrogen fixation by Trichodesmium in the central Atlantic Ocean, *Nature*, *411*(6833), 66–69, doi:10.1038/35075041.
Sarmiento, J. L., R. Slater, R. Barber, L. Bopp, S. C. Doney, A. Hirst, J. Kleypas, R. Matear, U. Mikolajewicz, and P. Monfray (2004), Response of ocean ecosystems to climate warming, *Global Biogeochem. Cycles*, *18*, GB3003, doi:10.1029/2003GB002134.
Savoie, D. L., Arimoto, R., Keene, W. C., Prospero, J. M., Duce, R. A., and Galloway, J. N. (2002), Marine biogenic and anthropogenic contributions to non-sea-salt sulfate in the marine boundary layer over the North Atlantic Ocean, *J. Geophys. Res.*, *107*(D18), 4356, doi:10.1029/2001JD000970.
Scanlan, D. J., and W. H. Wilson (1999), Application of molecular techniques to addressing the role of P as a key effector in marine ecosystems, in *Molecular Ecology of Aquatic Communities*, edited by J. P. Zehr and M. A. Voytek, pp. 149–175 , Springer, Netherlands.
Schulz, M., et al. (2012), Atmospheric transport and deposition of mineral dust to the ocean: Implications for research needs, *Environ. Sci. Technol.*, *46*(19), 10,390–10,404, doi:10.1021/es300073u.
Sedwick, P. N., E. R. Sholkovitz, and T. M. Church (2007), Impact of anthropogenic combustion emissions on the fractional solubility of aerosol iron: Evidence from the Sargasso Sea, *Geochem. Geophys. Geosyst.*, *8*, Q10Q06, doi:10.1029/2007GC001586.
Sholkovitz, E. R., P. N. Sedwick, T. M. Church, A. R. Baker, and C. F. Powell (2012), Fractional solubility of aerosol iron: Synthesis of a global-scale data set, *Geochim. Cosmochim. Acta*, *89*, 173–189, doi:10.1016/j.gca.2012.04.022.
Sohm, J. A., and D. G. Capone (2006), Phosphorus dynamics of the tropical and subtropical North Atlantic: Trichodesmium spp. versus bulk plankton, *Mar. Ecol. Prog. Ser.*, *317*, 21–28, doi:10.3354/meps317021.
Sohm, J. A., and D. G. Capone (2010), Zonal differences in phosphorus pools, turnover and deficiency across the tropical North Atlantic Ocean, *Global Biogeochem. Cycles*, *24*, GB2008, doi:10.1029/2008GB003414.
Sohm, J. A., C. Mahaffey, and D. G. Capone (2008), Assessment of relative phosphorus limitation of *Trichodesmium* spp. in the North Pacific, North Atlantic, and the north coast of Australia, *Limnol. Oceanogr.*, *53*(6), 2495–2502, doi:10.4319/lo.2008.53.6.2495.
Sohrin, Y., S. Urushihara, S. Nakatsuka, T. Kono, E. Higo, T. Minami, K. Norisuye, and S. Umetani (2008), Multielemental determination of GEOTRACES key trace metals in seawater by ICPMS after preconcentration using an ethylenediaminetriacetic acid chelating resin, *Anal. Chem.*, *80*(16), 6267–6273, doi:10.1021/ac800500f.
Srinivas, B., and M. M. Sarin (2013), Atmospheric deposition of N, P and Fe to the Northern Indian Ocean: Implications to C- and N-fixation, *Sci. Total Environ.*, *456*, 104–114, doi:10.1016/j.scitotenv.2013.03.068.
Steinacher, M., et al. (2010), Projected 21st century decrease in marine productivity: A multi-model analysis, *Biogeosciences*, *7*(3), 979–1005.
Steven, D. M., and R. Glombitz (1972), Oscillatory variation of a phytoplankton population in a tropical ocean, *Nature*, *237*(5350), 105–107, doi:10.1038/237105a0.
Subramaniam, A., et al. (2008), Amazon River enhances diazotrophy and carbon sequestration in the tropical North Atlantic Ocean, *Proc. Natl. Acad. Sci. U.S.A.*, *105*(30), 10,460–10,465, doi:10.1073/pnas.0710279105.
Sunda, W. G., and S. A. Huntsman (1992), Feedback interactions between zinc and phytoplankton in seawater, *Limnol. Oceanogr.*, *37*(1), 25–40.
Sunda, W. G., and S. A. Huntsman (1997), Interrelated influence of iron, light and cell size on marine phytoplankton growth, *Nature*, *390*(6658), 389–392, doi:10.1038/37093.
Thingstad, T. F., et al. (2005), Nature of phosphorus limitation in the ultraoligotrophic eastern Mediterranean, *Science*, *309*(5737), 1068–1071, doi:10.1126/science.1112632.
Trapp, J. M., F. J. Millero, and J. M. Prospero (2010), Temporal variability of the elemental composition of African dust measured in trade wind aerosols at Barbados and Miami, *Mar. Chem.*, *120*(1–4), 71–82, doi:10.1016/j.marchem.2008.10.004.
van der Werf, G. R., J. T. Randerson, L. Giglio, G. J. Collatz, P. S. Kasibhatla, and A. F. Arellano Jr. (2006), Interannual variability in global biomass burning emissions from 1997 to 2004, *Atmos. Chem. Phys.*, *6*(11), 3423–3441, doi:10.5194/acp-6-3423-2006.
Van Mooy, B. A. S., G. Rocap, H. F. Fredricks, C. T. Evans, and A. H. Devol (2006), Sulfolipids dramatically decrease phosphorus demand by picocyanobacteria in oligotrophic marine environments, *Proc. Natl. Acad. Sci. U.S.A.*, *103*(23), 8607–8612, doi:10.1073/pnas.0600540103.
Van Mooy, B. A. S., et al. (2009), Phytoplankton in the ocean use non-phosphorus lipids in response to phosphorus scarcity, *Nature*, *458*(7234), 69–72, doi:10.1038/nature07659.
Volpe, G., V. F. Banzon, R. H. Evans, R. Santoleri, A. J. Mariano, and R. Sciarra (2009), Satellite observations of the impact of dust in a low-nutrient, low-chlorophyll region: Fertilization or artifact?, *Global Biogeochem. Cycles*, *23*, GB3007, doi:10.1029/2008GB003216.
Voss, M., P. Croot, K. Lochte, M. Mills, and I. Peeken (2004), Patterns of nitrogen fixation along 10°N in the tropical Atlantic, *Geophys. Res. Lett.*, *31*, L23S09, doi:10.1029/2004GL020127.
Ward, D. S., S. Kloster, N. M. Mahowald, B. M. Rogers, J. T. Randerson, and P. G. Hess (2012), The changing radiative forcing of fires: Global model estimates for past, present and future, *Atmos. Chem. Phys.*, *12*(22), 10,857–10,886, doi:10.5194/acp-12-10857-2012.
Ward, D. S., N. M. Mahowald, and S. Kloster (2014), Potential climate forcing of land use and land cover change, *Atmos. Chem. Phys.*, *14*(23), 12,701–12,724, doi:10.5194/acp-14-12701-2014.

Williams, M. R., T. R. Fisher, and J. M. Melack (1997), Chemical composition and deposition of rain in the central Amazon, Brazil, *Atmos. Environ.*, *31*(2), 207–217.

Wu, J. F., W. Sunda, E. A. Boyle, and D. M. Karl (2000), Phosphate depletion in the western North Atlantic Ocean, *Science*, *289*(5480), 759–762, doi:10.1126/science.289.5480.759.

Wunsch, C., and P. Heimbach (2007), Practical global oceanic state estimation, *Physica D*, *230*(1–2), 197–208, doi:10.1016/j.physd.2006.09.040.

Wuttig, K., T. Wagener, M. Bressac, A. Dammshaeuser, P. Streu, C. Guieu, and P. L. Croot (2013), Impacts of dust deposition on dissolved trace metal concentrations (Mn, Al and Fe) during a mesocosm experiment, *Biogeosciences*, *10*(4), 2583–2600, doi:10.5194/bg-10-2583-2013.

Yu, H., et al. (2015), The fertilizing role of african dust in the amazon rainforest: A first multiyear assessment based on data from cloud-aerosol lidar and infrared pathfinder satellite observations, *Geophys. Res. Lett.*, *42*, 1984–1991, doi:10.1002/2015GL063040.

Zamora, L. M., J. M. Prospero, and D. A. Hansell (2011), Organic nitrogen in aerosols and precipitation at Barbados and Miami: Implications regarding sources, transport and deposition to the western subtropical North Atlantic, *J. Geophys. Res.*, *116*, D20309, doi:10.1029/2011JD015660.

Zamora, L. M., J. M. Prospero, D. A. Hansell, and J. M. Trapp (2013), Atmospheric P deposition to the subtropical North Atlantic: Sources, properties, and relationship to N deposition, *J. Geophys. Res. Atmos.*, *118*, 1546–1562, doi:10.1002/jgrd.50187.

Zhang, Y., L. Zheng, X. Liu, T. Jickells, J. N. Cape, K. Goulding, A. Fangmeier, and F. Zhang (2008), Evidence for organic N deposition and its anthropogenic sources in China, *Atmos. Environ.*, *42*(5), 1035–1041.